THE EFFECTS OF TARGET-DISTRACTOR COMPETITION ON THE OCULOMOTOR SYSTEM

CAROLINE GIURICICH

A THESIS SUBMITTED TO THE FACULTY OF GRADUATE STUDIES IN PARTIAL FULFILLMENT OF THE REQUIREMENTS FOR THE DEGREE OF MASTER OF SCIENCE

GRADUATE PROGRAM IN KINESIOLOGY AND HEALTH SCIENCE

YORK UNIVERSITY

TORONTO, ONTARIO

AUGUST 2021

Abstract

We use our eyes to investigate the world around us and decide what we want to act on. In a crowded scene, we direct our gaze to a single object of interest to gather more information about it. We do this effortlessly, but the underlying neural circuitry is complex. In this thesis, I look at temporal, spatial, and object identity factors that feed into the oculomotor system to drive eye movements in a target selection task. We varied the distance and similarity of complex objects to examine the effects of target-distractor competition on saccade trajectories and pupil size. We found that the effects of distance and similarity on saccade trajectories depended on the development of target-distractor competition. However, these factors did not modulate pupil size. Overall, these findings show that information processed in higher order visual areas is projected to the oculomotor system for saccade planning but not pupillary control.

For Mom

Look how far I've come!

Acknowledgments

To start off, I'd like to give a huge thank you to my supervisor Dr. Mazyar Fallah. Thank you for teaching me about the world of eye movements and for having an answer to every question I ask, no matter how many there are. You've always been very kind, light-hearted, and approachable. I appreciate all the help, advice, support, and encouragement you've given me since day one, and I'm so grateful to have gotten the opportunity to do my master's under your supervision. Thank you so much!

I'd also like to give a special shoutout to Dr. Denise Henriques for being a great supervisory committee member amongst many other things. Thank you for all your help and enthusiasm throughout these past two years!

To my lab mates from The Visual Perception and Attention Lab: thank you for all the insight and advice about research and academia. I wish we could have spent more time together chatting, laughing, and telling stories in and outside of the lab. Special mentions to Rob and Heather for your expertise and for helping me learn the ins and outs of research. As well, a big thank you to the friends I made at York, especially from the Neuroscience Graduate Diploma Program. I couldn't have navigated through graduate school life without you, and I can't wait to finally see you all again!

To my friends and family: thank you for having my back from the beginning and for taking my mind off school when I need a break. I'm so lucky to have such an amazing support system. Special shoutout to Cameron: thank you for your endless love and support in everything I do. You're always there when I need a shoulder to cry on, a good laugh, or someone to rant to about how stressed I am, and I appreciate you so very much.

Table of Contents

List of Tables

List of Figures

Chapter 1: Introduction and The Visual System

1.1 Introduction

Vision is one of the most well-researched senses and arguably one of the most important to study. It allows us to make sense of the world around us and evaluate what is worth acting on. In the natural environment, our visual fields are crowded and full of potential objects to view and learn more about. Often in these crowded scenes, multiple objects are competing for our attention since it is only possible to direct full attention to one object at a time. It is necessary for us to make decisions and resolve this competition about what in our visual field is most important to act on to better understand and efficiently interact with our environment. We use eye movements, such as saccades, to gather information and focus on objects of interest. The eye movements we make encode information about the scene being viewed, the competition between objects, and our oculomotor decisions. Examining this behaviour provides a gateway to understanding the diverse set of neural mechanisms involved. Two overarching neural circuits are the visual system and the oculomotor system. Although there are interactions between the structures of each system, they can individually be characterized as being responsible for processing visual stimuli and creating motor plans to act on these stimuli, respectively. In the following thesis, I will discuss the effects of object competition on dynamic and fixational eye movements and the underlying neural circuitry. To start, I will give a review of the anatomy and function of the visual and oculomotor systems, followed by a look into oculomotor encoding and saccade curvature, and finishing with a brief overview of the literature on pupillometry.

1.2 The Visual System

The visual system begins at the retina and ends at areas of higher order visual processing. It diverges into two pathways, the dorsal and ventral streams, which control the processing of distinct visual information. In the following section I will give an overview of the two streams through discussing their basic anatomy and function.

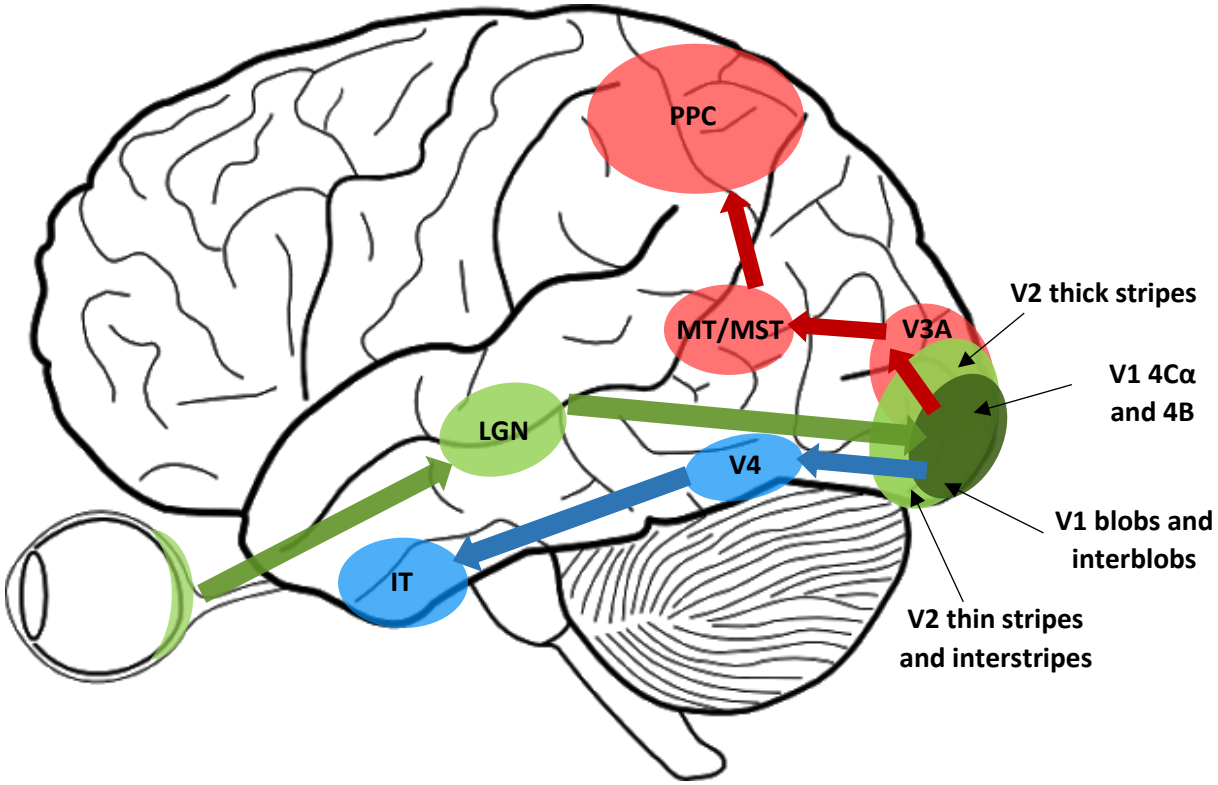

Figure 1.1. The visual system hierarchy and major structures of the dorsal and ventral streams. This diagram depicts the flow of visual information from the retina to the lateral geniculate nucleus (LGN) to V1, as shown in green. It further illustrates the dorsal and ventral streams that project from separate layers of V1 to higher order areas of visual processing. The dorsal stream is shown in red, and the ventral stream is shown in blue.

1.2.1 Magnocellular and Parvocellular Pathways

The visual information collected by the retina is split into two main ganglion cell groups: magnocellular (M) and parvocellular (P). M cells transmit motion information and have large receptive fields, whereas P cells have smaller receptive fields and are mostly responsible for transmitting more detailed stimulus information such as colour and form (Zeki, 1973; DeYoe & Van Essen, 1988; Livingstone & Hubel, 1988). The respective information is transmitted to the M and P layers of the LGN, which further project to V1. The pathways remain separated through V1 where M cell information is processed in layers 4Cα and 4B, and P cell information is processed in the blob and interblob layers (4Cβ). The distinct V1 layers pass information forward to V2 where the M pathway continues through the thick stripes and the P pathway through the thin stripes and interstripes. This anatomical divide of the M and P pathways creates the dorsal and ventral streams, respectively, which further project from V2 to separate areas of the visual cortex and regions of higher order processing (Figure 1.1).

1.2.2 The Dorsal Stream

The dorsal stream of visual processing, also termed the 'How' pathway, has been categorized as the pathway for 'vision for action' (Goodale & Milner, 1992). Originating in V1, this pathway makes its way through V2, V3A, V5/middle temporal area (MT), medial superior temporal area (MST), and ends at the posterior parietal cortex (PPC). The visual information encoded by magnocellular cells of the retina and layers of the LGN is primarily projected and processed throughout this pathway (Kafaligonul, 2014). V1 is retinotopically mapped (each point of the visual field is topographically represented in the cortex) and is responsible for processing simple features such as orientation and direction of motion (Horton & Hoyt, 1991). Following the hierarchy of nodes of the dorsal stream, receptive field size increases along with increasing

complexity for processed visual features. For the dorsal stream, layers 4Cα and 4B of V1 primarily carry magnocellular input forward to the thick stripes of V2 (Hubel & Wiesel, 1972; Dow, 1974). These layers of V2 are also selective for orientation, motion direction, and depth information and further project to V3A and MT (Shipp & Zeki, 1985; Shipp & Zeki, 2002; Dow, 1974). Being that MT is further along the visual hierarchy, it is specialized for more complex motion processing such as motion aftereffects, global motion, and pattern motion (Tootell et al., 1995; Huk et al., 2001; Castel-Branco et al., 2002; Huk & Heeger, 2002). MT projects to MST which has neurons specialized for specific types of motion, such as translation and rotation, and is also involved in illusory motion and optic flow (Sakata et al., 1994; Saito et al., 1986; Ichikawa et al., 2006; Duffy, 1998; Pan et al., 2016). MST further projects to the PPC which is involved in a variety of types of visuospatial processing such as spatial navigation and control of action (for a review, see Kravitz et al., 2011). Taken together, the dorsal stream is involved in both the location of stimuli of interest in the visual field and how we plan on acting on them, whether it be through manual reaching and grasping, or eye movements (Milner & Goodale, 2008).

1.2.3 The Ventral Stream

The ventral stream of visual processing has been termed the ‘What’ pathway and is involved in ‘vision for perception’ (Goodale & Milner, 1992). In contrast to the dorsal stream, the ventral stream specializes in more detailed, intrinsic stimulus information necessary for perception of the object, rather than creating motor plans to act on the object. The pathway also begins in V1 where the information from the parvocellular layers of the LGN is projected (Hubel & Wiesel, 1972; Lund & Boothe, 1975). Similar to the dorsal stream, receptive field size increases throughout the hierarchy of the ventral stream, and the features encoded become more

complex from V1 to the final structures of this pathway, including the inferior temporal (IT) cortex. Layer 4Cβ of V1, or more specifically the blob and interblob layers, is tied to ventral stream processing and carries dominantly parvocellular visual information through to V2 (Hubel & Wiesel, 1972). The blob layers of V1 carry information about colour whereas the interblob layers carry information about orientation (Hubel & Wiesel, 1962; Livingstone & Hubel, 1984; Hubel & Livingstone, 1987). Respectively, they output to the thin stripe and interstripe layers of V2 which project colour and form information to V4 (Shipp & Zeki, 1985; Shipp & Zeki, 2002; Felleman et al., 1997). This is where colour perception begins and where curves and simple shapes are processed (Zeki, 1973; Roe et al., 2012; Pasupathy & Connor, 1999; Tang et al., 2020). V4 feeds forward into the IT cortex where more complex visual processing occurs. The IT cortex is capable of processing complex shapes and objects and is also involved in object recognition (Baylis & Rolls, 1987; Miller et al., 1993). Higher up structures in the ventral stream become more specialized, such as the fusiform face area that is active when viewing faces, and the extrastriate body area responsible for identifying body parts (Kanwisher et al., 1997; Downing et al., 2001). Altogether, the ventral stream is important for perception of the objects and stimuli around us.

Chapter 2: The Oculomotor System

The oculomotor system plays a large role in vision through preparing and executing saccadic eye movements. In the following section, I will start with a brief review of the anatomy and function of three main regions of the oculomotor system: the brainstem, the superior colliculus (SC), and the frontal eye field (FEF) (Figure 2.1). I will then discuss oculomotor planning and how it relates to the SC and FEF with respect to winner-take-all models and priority maps. This will be followed by an overview of saccade curvature and target-distractor competition. Lastly, I will give a brief introduction to pupillometry, the study of pupil size, and its relation to visual attention.

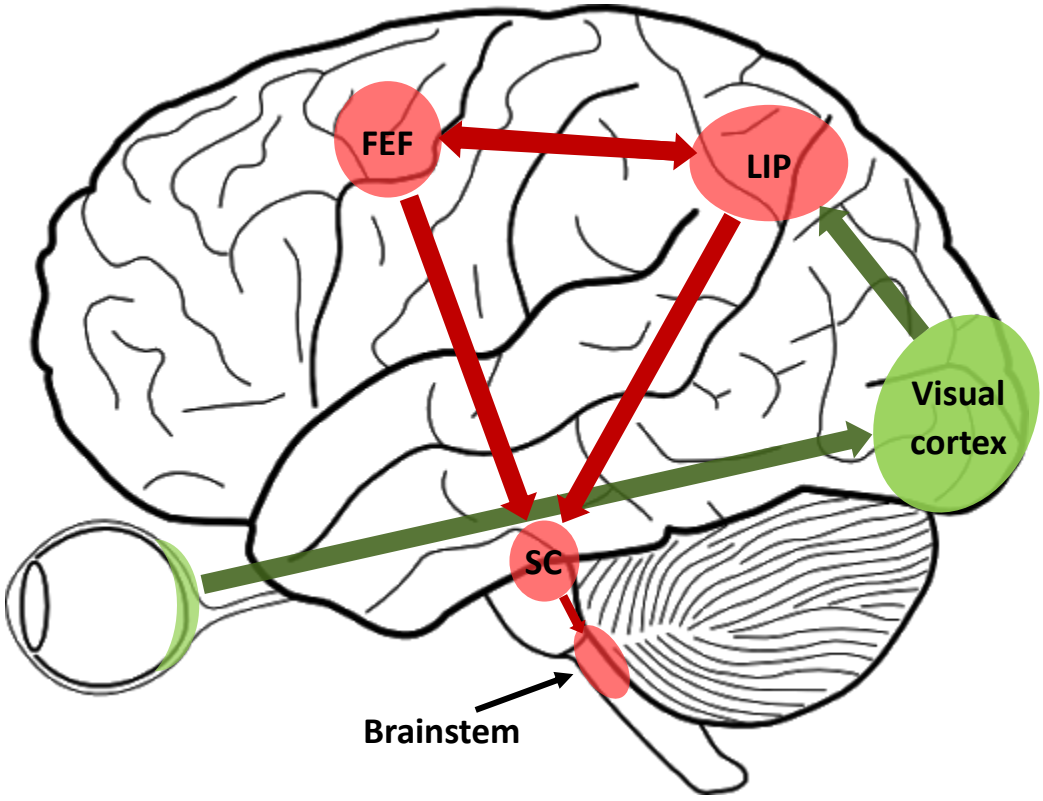

Figure 2.1. Anatomical structures and connections of the oculomotor system in relation to saccadic eye movements. This diagram highlights the major connections between structures of the oculomotor system. Acronyms of structures not discussed in the text: lateral intraparietal area (LIP).

2.1 The Brainstem

The brainstem is involved in saccadic eye movements through the activation of the extraocular muscles of the eye. Horizontal and vertical eye movements are controlled through three motor nuclei (abducens, oculomotor, and trochlear) that innervate the six extraocular muscles (for a review, see Sparks, 2002). Premotor neuron activity correlated to horizontal saccades is found in the paramedian pontine reticular formation (PPRF) and medulla (Cohen & Komatsuzaki, 1972). Premotor activity in the rostral interstitial nucleus of the medial longitudinal fasciculus (riMLF) controls vertical saccades (Buttner et al., 1977; Buttner-Ennever & Buttner, 1978; King et al., 1981). Burst neurons found in the PPRF and riMLF increase activity before saccade initiation (pulse) whereas other neurons maintain the saccade while it is happening (step) (Igusa et al., 1980; Strassman et al., 1986; Spencer et al., 1989). On the other hand, omnipause neurons are necessary for fixation; they are active during fixation before a saccade through inhibiting excitatory neurons, are inhibited during the saccade, and reactivate before the end of the saccade to prepare for post-saccade fixation (Cohen & Henn, 1972; Evinger et al., 1982; Optican 2008). Saccades that are not exclusively horizontal or vertical occur with the help of pontine omnipause neurons that synchronize the horizontal and vertical burst neuron onsets through inhibition to create a more coordinated saccade (Curthoys et al., 1984). Although the onsets of these burst neurons are synchronized, the offsets are not, which gives rise to a curved saccade (Sparks, 2002).

2.2 The Superior Colliculus

The superior colliculus (SC) is a layered structure located in the midbrain of the brainstem. It is primarily involved in vision but is also important for other sensory processes, such as audition. More specifically, the SC plays a large role in visual attention and target

selection (Ignashchenkova et al., 2004; Krauzlis et al., 2013; McPeek & Keller, 2002; White & Munoz, 2011). The layers of the SC are often divided into the superficial or visuosensory layers, and the intermediate and deep, or motor layers. The visuosensory layers are found in the dorsal SC and receive visual information from the retina, whereas the motor layers are more ventrally located and are involved in orienting movements such as saccades (Schiller, 1984). The visuosensory layers receive inputs from structures of the visual system including the retina, LGN, striate (V1) and extrastriate (V3, V4, MT) cortices (Schiller, 1984). The visuosensory layers have outputs to the LGN and pulvinar nuclei of the thalamus (Albano et al., 1979; Harting et al., 1991). The motor layers have a vast array of inputs spanning the brain including structures found in the parietal cortex, cerebellum, medulla, pons, midbrain, and even the spinal cord (Andersen et al., 1985; Edwards et al., 1979). These deeper layers project to nuclei of the thalamus, pons, and central nervous system (Edwards et al., 1979). As well, the SC's role in vision can be tied to the brainstem pulse-step generators, since its output projections lead to the PPRF and riMLF premotor areas (Sparks & Hartwich-Young, 1989).

Early research of the SC found that it topographically maps the visual field through retinal projections, where the left and right hemifields map to contralateral sides of the SC (Apter, 1945; Hess et al., 1946). The visuosensory and motor layers of the SC have been found to function using separate maps that encode different forms of visual information from the visual field. The visuosensory layers map the location of visual stimuli in space (Goldberg & Wurtz, 1972), whereas the motor layers map saccadic eye movements and where they are made in the visual field, also referred to as 'movement fields' (Wurtz & Goldberg, 1972; Robinson 1972). In addition to the motor map in the intermediate and deep layers of the SC, the dual coding hypothesis was posited which states that the speed and vector (amplitude and direction) of the

upcoming saccade can be read out from the frequency of bursts and the location of this neural discharge from the motor neuron population, respectively (Sparks & Mays, 1990; Rohrer et al., 1987). Taken together, the sensory and motor maps of the SC communicate to produce sensorimotor integration resulting in voluntary or reflexive oriented saccadic eye movements towards stimuli (Lee et al., 1997; Hall & Moschovakis, 2003). Volitional saccades would be influenced by top-down control. Reflexive saccades towards an unexpected stimulus could involve multisensory integration, where a flash of light or a loud noise could cause an oriented eye movement developed by the SC.

2.3 The Frontal Eye Field

The frontal eye field (FEF) is a structure of the oculomotor system not in the brainstem. It is located along the precentral sulcus, near the superior frontal sulcus. The FEF has input connections from the supplementary eye field, parietal eye field, principal sulcus, MT, and substantia nigra (Schall et al., 1993; Tian & Lynch, 1996). It has output projections to the prestriate (V2) and extrastriate cortices as well as subcortical regions such as the pons, basal ganglia, and some thalamic nuclei (Stanton et al., 1993; Stanton et al., 1995; Leichnetz et al., 1984; Segraves, 1992; Stanton et al., 1988). In addition to these connections, the FEF has reciprocal connections with the lateral interparietal area, parietal cortex, and importantly, the SC (Stanton et al., 1995; Tian & Lynch, 1996; Huerta et al., 1987; Cavada & Goldman-Rakic, 1989).

The FEF is involved in the preparation and initiation of eye movements. It controls various types of eye movements, such as saccades, fixation, and smooth pursuit (Bizzi, 1986; Bruce & Goldberg, 1985; Izawa et al., 2004, 2009). When it comes to saccades, many studies link the role of the FEF to voluntary saccades more than reflexive saccades (Robinson, 1968). For instance, prefrontal cortex lesion and transcranial magnetic stimulation studies have shown

that the FEF is necessary for executing voluntary saccades during endogenous saccade tasks (Henik et al., 1994; Ro et al., 1997; Vernet et al., 2014; Muri & Nyffeler, 2008). Similar to the SC, the FEF has been found to function using topographically organized maps which encode saccade direction and amplitude (Robinson & Fuchs, 1969; Bruce et al., 1985). Moving from lateral to medial FEF increases the amplitude of the saccade vector, whereas moving down the precentral sulcus in depth changes the angle/direction of the saccade vector (Robinson & Fuchs, 1969; Bruce et al., 1985; Tehovnik et al., 2000). When moving down the precentral sulcus at the same medial-lateral location, the angle of the saccade vector changes, but the amplitude of the saccade vector remains constant (isoeccentric saccades) (Figure 2.2).

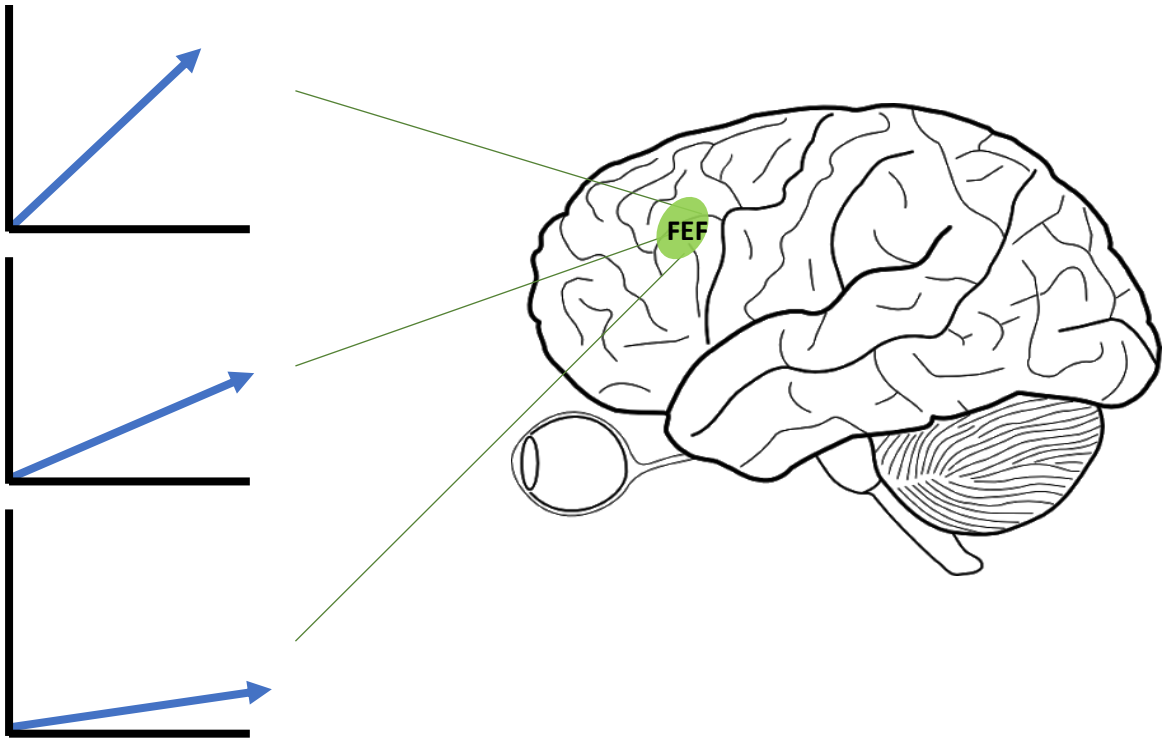

Figure 2.2 Topographically organized map in the FEF codes saccade amplitude and direction. The blue arrows represent the saccade vector outputted after stimulation of the FEF. Moving down the precentral sulcus in depth gives rise to different vector angles. Vectors are constant in amplitude if the same medial-lateral location of the FEF is stimulated.

2.4 Oculomotor Plans and Encoding

Saccadic eye movements allow us to process stimuli in the world around us quickly and efficiently. We direct our gaze at a single object of interest amongst other objects in a scene to enhance its processing in the brain at a cost to the other objects (James, 1890). There are many factors that come into play when making oculomotor plans during a target selection task and resolving this competition for attention, most of which fit into two broad categories: bottom-up and top-down factors. Bottom-up factors involve the physical features and salience/distinctiveness of the objects themselves, such as colour, shape, and orientation (Wolfe,

1992, 1994). Top-down factors come from cortical signals and take the viewer's goals and the relevance of the stimuli into consideration (Colby & Goldberg, 1999; Desimone & Duncan, 1995; Reynolds & Chelazzi, 2004; Roelfsema, 2006). With selective attention, when a saccade is directed towards the stimulus that catches the most attention, it is called 'winner-take-all' (Feldman, 1982; Koch & Ullman, 1985; Tsotsos et al., 1995; Itti & Koch, 2001). A saliency map encodes the weighted saliency of the stimuli across the visual field and the most salient spot on the map is the location to which the saccade will be directed (Findlay & Walker, 1999; McIlwain, 1986). This 'winner' is the population of neurons with the most neural activity at the time of movement initiation which encodes the location of the salient stimulus (Findlay & Walker, 1999). Some models of saccade planning are based solely on saliency, but the top-down/cortical effects play a role as well. A priority map combines both the saliency and the relevance of the stimuli in question to create a better representation of oculomotor planning (Wolfe 1994; Serences & Yantis, 2006; Fecteau & Munoz, 2006).

The SC and FEF are heavily involved in visual search/discrimination, and neural activity in these areas has been shown to be consistent with saliency and/or priority maps. A study by White et al. in 2017 demonstrated through computational modelling and neuron recordings from primate SC during a free viewing task that activity in the superficial, visuosensory layers of the SC is consistent with a saliency map. In contrast, they discussed that the intermediate, motor layers of the SC are more likely compatible with a priority map due to its connections with the FEF. Although the existence of a saliency map in the FEF is well studied (Walker et al., 2009; for a review, see Thompson & Bichot, 2005), a study by Fernandes et al., (2013) examined the role of the FEF in a natural scene search task and concluded that FEF neuron activity is weakly dependent on a saliency map solely encoding bottom-up features. Instead, they suggested that the

FEF primarily encodes saccade planning and movement information. Therefore, both the SC and FEF are important for target selection tasks, and the patterns of neural activity in each gives us information about subsequent saccadic eye movements.

FEF neurons can be classified as motor, visuomotor, or visual (Bruce & Goldberg, 1985; Costello et al., 2013). When planning to saccade to a target inside the receptive field, the respective motor burst neurons increase activity from a baseline level until activity peaks above threshold, leading to saccade onset (Figure 2.3A) (Hanes & Schall, 1996; Heitz & Schall, 2012; Steinmetz & Moore, 2012; Thompson et al., 1997). After a target onsets inside the receptive field, visuomotor neurons increase activity (Fig 2.3B). Another, more robust wave of activity is seen leading up to saccade onset. When planning a saccade to a target outside of the receptive field, motor and visuomotor neurons show less activity. Motor neurons remain at baseline levels of activity from target onset through to saccade initiation (Fig 2.3A), whereas visuomotor neurons show an increase in activity after target onset. This wave of neural activity peaks below that of the target-in response, then decreases to baseline prior to saccade onset (Fig 2.3B). The activity of visuomotor neurons when planning saccades to stimuli in (target) or out (distractor) of the receptive field is representative of target-distractor competition. If this competition has not been resolved by the time of saccade onset, the saccade would be initiated closer to target-distractor onset when peaks in neural activity for both objects occur. If target-distractor competition has completed, the saccade would be initiated as depicted in Figure 2.4B, and the neural activity encoding the distractor decreases below threshold by the time of saccade initiation. These differences in neural activity encoding each object results in saccade deviation towards versus away from the distractor, as will be further introduced in the following section.

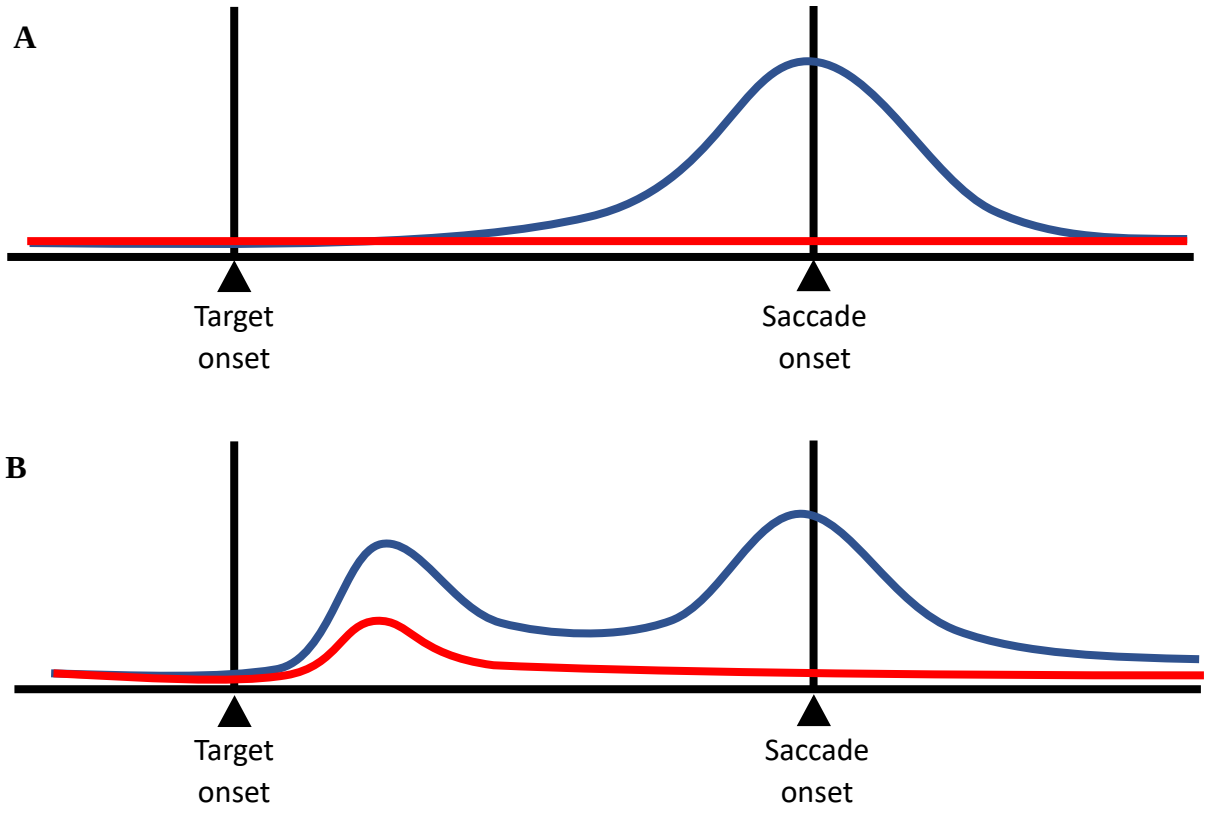

Figure 2.3. Activity of FEF motor and visuomotor burst neurons from target onset to saccade onset. Blue curves represent the firing rates of burst neurons responding to target onset inside the receptive field. Red curves represent the firing rate of burst neurons responding to target onset outside the receptive field. *A*: Motor neuron activity. *B*: Visuomotor neuron activity. Adapted from Costello MG, Zhu D, Salinas E, Stanford T. Perceptual modulation of motor – but not visual – responses in the frontal eye field during an urgent-decision task. *J Neurosci* 33: 16394-16408, 2013. doi: 10.1523/JNEUROSCI.1899-13.2013. For the full article, see https://www.jneurosci.org/content/33/41/16394.

2.5 Saccade Curvature

When making a saccadic eye movement to a target object, if the target is the only object on the display, the eye movement made will be relatively straight and will follow the direct path to the target (Bahill & Stark, 1977; Keller, 1980; King et al., 1986; Quaia et al., 2000; Van Gisbergen et al., 1985; Viviani et al., 1977). When there are multiple objects on the display, such

as a target and distractor object, previous research has shown that both objects will compete for attention and the saccade will curve towards the distractor (Findlay & Harris, 1984; McPeek & Keller, 2001; Minken et al., 1993; Port & Wurtz, 2000; Van Gisbergen et al., 1987). McPeek et al. demonstrated using neuron recordings and stimulation, that this curvature due to competing saccade goals occurs due to differences in neural activity in the SC (2003) and/or the FEF (McPeek, 2006). For both the SC and FEF, separate sets of neurons encode each object of the visual search task and during the time immediately prior to saccade initiation, the activity in each population continues to compete for dominance (McPeek et al., 2003; McPeek, 2006). Curvature towards the distractor is indicative of the distractor's ability to capture gaze (Figure 2.4A), but curvature away from the distractor can occur with more time before saccade initiation (Figure 2.4B). In a task involving target and distractor objects, a delay was introduced before saccade initiation could occur (Godjin & Theeuwes, 2004). It was shown that with more time before making a saccade, the participants could fully cortically process the objects and inhibit the neural activity encoding the distractor resulting in saccade trajectories curved away from the distractor (Godjin & Theeuwes, 2004). Walker et al. showed that other factors can affect saccade curvature direction, such as prior knowledge of the target location, which aids the target selection process and results in curvature away from the distractor as well (2006).

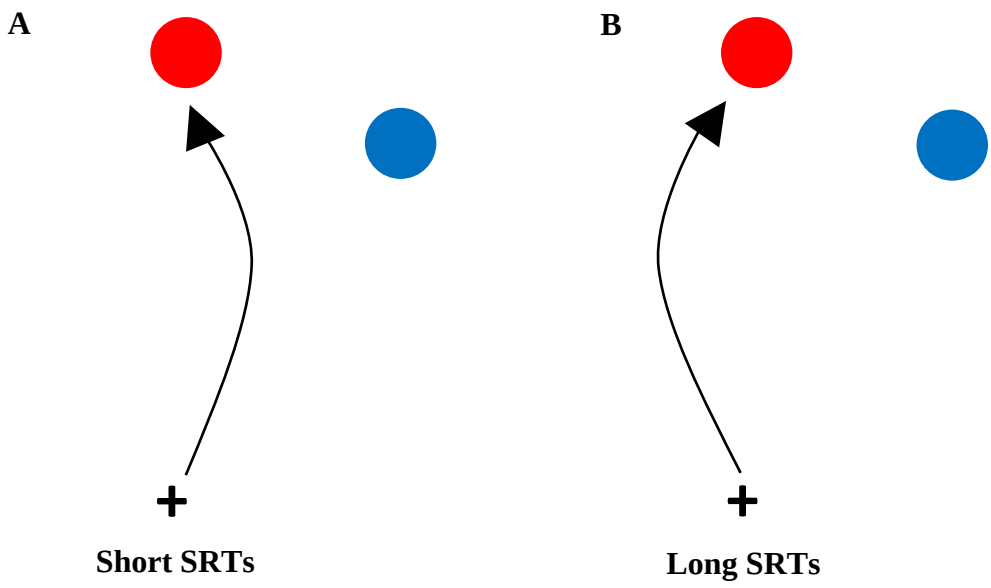

Figure 2.4. Saccades made at short and long saccadic reaction times (SRTs) from target-distractor onset. The target is depicted by the red circle and the distractor is depicted by the blue circle. *A*: Saccades curve towards the distractor at short SRTs. *B*: Saccades curve away from the distractor at long SRTs.

The time before saccade initiation and prior knowledge of target locations affect the amount and direction of saccade curvature in a target selection task, but so can the common features/similarity between the objects. The similarity between the target and distractor is an example of behavioural relevance, which is a combination of bottom-up and top-down features. Many studies have examined the effects of simple feature similarity on saccade curvature, especially using stimuli with lower order features such as colour and orientation. For instance, studies by Mulckhuyse et al. (2009) and Ludwig & Gilchrist (2003) used colour congruency as the measure of similarity between a target and distractor. They showed that when the target and distractor colour is congruent, the saccade curves more towards the distractor compared to when they are colour incongruent. These effects observed with simple features have been shown to extend to studies manipulating the similarity between higher order, complex objects. An example

is a study by Kehoe et al. (2018a) where the similarity of complex objects composed of line segments was varied. They found that similarity and saccade curvature follow a linear relationship, where more saccade curvature is seen with more line segment differences between objects; the less similar they are, the more the distractor can be suppressed from attention (Kehoe et al., 2018a). Therefore, target-distractor competition has a large effect on saccade trajectories when either simple or complex stimuli are used, but tasks involving these higher order objects are important to study to learn more about competition between stimuli in the real world.

To quantify the amount of saccade trajectory deviation from target-distractor competition, a variety of saccade metrics are often used (Figure 2.5). The most common are initial angle, endpoint deviation angle, sum curvature, max curvature, and angle at max curvature. Initial angle is calculated as the angle between the point at 20% along the length of the saccade trajectory to the vertical axis connecting the starting point to the target location. Endpoint deviation angle is the angle between the final point of the saccade and the vertical axis to the target. The three curvature metrics require the saccade to be rotated so that the final point of the saccade lies on the vertical axis. Sum curvature is the sum of all horizontal deviations from the vertical axis. Max curvature is the value of horizontal deviation from the most deviated point along the saccade. Angle at max curvature is the angle from the most deviated point to the vertical axis. Based on these calculations, positive values for each metric represent deviations towards the distractor whereas negative values represent deviations away from the distractor. These metrics thoroughly describe the saccade trajectory shape and aid in analysis of target-distractor competition.

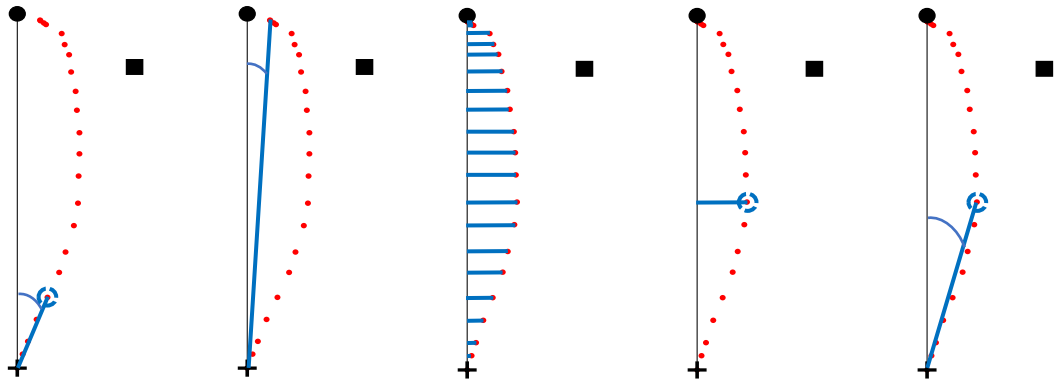

Figure 2.5. Saccade deviation metric calculations. Metrics from left to right: initial angle, endpoint deviation angle, sum curvature, max curvature, angle at max curvature. The target and distractor are represented by a black circle and square, respectively. Red points depict the eye position every 2ms from saccade start at the fixation cross to end at the target. The right three metrics are calculated with the saccade rotated so the final point lies on the vertical axis.

As mentioned above, various factors can affect saccade curvature, and thus the saccade metrics, including object similarity and colour (Kehoe et al., 2018a, b). The effects of these variables on saccade metrics often follow patterns commonly found in neuroscience. There are a variety of functions that have been observed or used to model brain behaviour, often in the visual system. Neural circuits tend to be repeated throughout the brain for various behaviours, especially cortically. Thus, it is likely that patterns observed for one neural circuit may be observed for another, where both are modelled by the same function. Linear patterns are seen when neuronal firing rates scale with stimulus intensity. An example is in the auditory system with the logarithmic decibel scale, commonly modelled linearly when using a log-scale; perceived loudness increases linearly on a log-scale as decibels increases. As well, a study showed that auditory spatial cues are processed linearly by primary auditory cortex neurons (Schnupp et al., 2001). Sigmoid patterns showing an asymptote or level of saturation can be

observed when modelling contrast response functions in the early visual system as well as in MT (Fallah & Reynolds, 2012). A study by Fallah and Reynolds (2012) showed that the oculomotor gain of eye velocity during smooth pursuit saturated at low levels of luminance contrast, modelled with a sigmoid curve. Exponential curves commonly model motion sensitive neurons, such as in MT. Studies have shown that neurons adapt to stimulus motion over time, where the perceived speed of a stimulus moving at a constant speed reduces exponentially as motion duration increases (Bex et al., 1999; Hammett et al., 2000; Price & Born, 2009). Gaussian curves are often used to model featural or orientation selectivity and selective tuning in V1 (Butts & Goldman, 2006; Jeon et al., 2018). A more complex way to model selective tuning is using a Difference of Gaussian (DoG) function. They are also commonly used in the divisive normalization model of attention showing surround suppression found in early visual processing areas such as V2 and V4 (Reynolds & Heeger, 2009; Tostsos, 1990; Tsotsos et al., 1995; Kehoe et al., 2018b). A sharper-tuned excitatory Gaussian combined with a broader-tuned inhibitory Gaussian create a DoG shape, which fits with the patterns of inhibition surrounding an attended item found in spatial attention.

2.6 Pupillometry

Pupillometry is the study of pupil size. When there is more light entering the eye, the pupil constricts; when there is less light, the pupil dilates (Hakerem, 1967). This pupillary light reflex is mediated subcortically. Luminance-sensing ganglion cells of the retina carry light information to cranial nerve nuclei which produce the subsequent pupillary response (Loewenfeld, 1993; Gamlin et al., 1995).

Changes in pupil size can also be attributed to cognitive workload and attention (Laeng et al., 2012). Single cell recordings have shown that activity in locus coeruleus neurons correlates

to pupil size during tasks requiring cognitive load (Rajkowski et al., 1993; Rajkowski et al., 2004). When a task is more difficult or requires more attention, the pupil dilates for better focus (Laeng et al., 2012; Hess & Polt, 1964). An example of such a task is mental math. In a study by Hess and Polt (1964), participants were instructed to mentally calculate multiplication problems and say their answer out loud. They showed that pupil size increased with increasing difficulty of mental multiplication. Control of the pupil has been shown to be affected top-down by the oculomotor system. For instance, a study by Ebitz & Moore (2017), demonstrated the role the FEF plays in pupil size. They microstimulated regions of the FEF and found that a stimulus flashed within the receptive field of the stimulated FEF neurons would cause a pupillary response. Although pupillometry with respect to cognitive load and attention has been thoroughly researched (Lehmann & Corneil, 2016; Wang et al., 2012; Wang et al., 2015; Ebitz & Moore, 2017; Wang et al., 2014; Ebitz & Moore, 2019), it has not been looked at in relation to competition between objects in a priority map, specifically when varying the similarity and/or spacing of competing objects.

Chapter 3: Goals and Hypotheses

The following chapters examine the effects of target-distractor competition on saccades, and pupil size during a delayed match to sample task involving a visual search for a previously shown target. Our goal for these studies was to determine the effects of varying similarity and angular distance of a target and distractor on saccade trajectories and see if these results can be replicated through pupil size during the period of fixation prior to saccade initiation. We set out to address the following questions and hypotheses:

1. How does varying angular distance between a distractor and the saccade target affect saccade trajectory shape? We hypothesized that if the target-distractor competition process is incomplete by the time of saccade initiation, angular distance would modulate saccade trajectories through weighted vector averaging. With enough time to resolve the competition, we expected that angular distance would modulate saccade trajectory following the pattern of a spatial suppressive surround.

2. How does varying the similarity of complex target and distractor objects affect saccade trajectory shape? We expected that if an object-based suppressive surround exists, as does for simple features, we would find evidence of it through the effects of similarity on saccade trajectory.

3. Do the angular distance and similarity between a target and distractor interact? Since we are varying the target-distractor distance and similarity simultaneously, we expected that these variables would interact to produce the observed effects on saccade trajectories.

4. How does the timing of the competitive interactions between target and distractor, as measured by saccadic reaction time, affect saccade trajectories and interact with the manipulated variables? We hypothesized that more time to resolve target-distractor competition would be necessary to inhibit the distractor more. We expected that distractor inhibition would affect saccade trajectory shape through angular distance and similarity.

5. Will the effects of angular distance and similarity on saccade trajectories be reflected in pupil size within a period of fixation after target-distractor onset and before saccade initiation? Resolving the target-distractor competition is more difficult when the objects are more similar and farther away from each other. We expected that with these more difficult task conditions, pupil size would dilate. Additionally, we hypothesized that developing oculomotor plans, related to covert spatial attention and priority maps, would be reflected in pupil size.

Most studies examining the effects of similarity on saccade curvature have kept the distractor at a set distance to the target. As well, objects with simple features are often used rather than more complex objects, such as those used in Kehoe et al. (2018a). Previous research has shown that spatial suppressive zones surround a spotlight of attention centered at a target object, resulting in the inhibition of stimuli falling within the suppressive zone. Similar suppressive surrounds have been found in feature-space for simple features such as colour, orientation, and direction of motion, but it is unclear if a suppressive surround in object-space exists. Through a target selection task where the distance and similarity of complex objects was varied

simultaneously, we aimed to better understand the effects of target-distractor competition on saccade metrics. As well, we were interested in the potential interactions of angular distance and similarity and the timing of the target-distractor competition process as observed through the effects of these variables on saccade trajectories. Hypotheses 1-4 are addressed in the manuscript in Chapter 4.

The relationship between cognitive load and pupil size has been thoroughly studied, especially using simple features such as luminance. Examining the changes in pupil size when resolving target-distractor competition between complex objects is novel to the field. The oculomotor system is involved in this competition process through creating saccade motor plans with respect to covert spatial attention and priority maps. Previous studies showing effects of FEF stimulation on pupillary responses give neurophysiological evidence of pupillary changes to the oculomotor system. This suggests a relationship between target-distractor competition and pupillometry, which is examined through hypothesis 5 in Chapter 3.

Chapter 4: Target-distractor competition modulates saccade trajectories (Manuscript)

This manuscript will be submitted to the ***Journal of Neurophysiology***. The co-authors of this manuscript are Dr. Robert Green, Dr. Heather Jordan, and Dr. Mazyar Fallah. Caroline Giuricich and Dr. Fallah designed the experiment. Caroline Giuricich ran the experiment and collected the data. Caroline Giuricich analyzed the data with input from Dr. Green, Dr. Jordan, and Dr. Fallah. Caroline Giuricich wrote the manuscript with feedback from all co-authors.

4.1 Abstract

Recent studies have shown that the similarity between nearby target and distractors affects the curvature in saccade trajectories, likely due to target-distractor inhibition. In this study, we varied the distance between, as well as the similarity of complex target and distractor objects in a delayed match to sample task to examine their effects on saccade trajectories and better understand the underlying neural circuitry. For trials with short saccadic reaction times (SRTs), the effect of distance was consistent with saccade vector averaging, whereas the effect of similarity suggested the existence of an object-based suppressive surround. At longer SRTs, there was sufficient time for competition between the objects to fully develop and saccade curvature was modulated by the target-distractor distance, exhibiting the effects of a spatial suppressive surround. In contrast, as the target-distractor similarity decreased, the initial saccade angle away from the distractor increased, reflecting stronger distractor inhibition. There were no significant interactions between distance and similarity. Taken together, the stage of the target-distractor competition process at which a saccade was initiated determined the independent effects of distance and object similarity on saccade trajectories. Furthermore, these results suggest that target-distractor interactions can be intrinsically measured from the saccade trajectory.

4.2 New and Noteworthy

We show that the effects of distance and object similarity on saccade trajectories are independent of each other but are themselves driven by the target-distractor competition process. Thus, spatiotemporal and object identity factors feed into saccade planning and execution, resulting in modulations of the saccades' metrics. These findings are important for understanding

the dynamic networks guiding target selection and are relevant for further development of eye-tracking applications in health and disease.

4.3 Introduction

When there are two potential saccade goals in the environment, both objects compete for attention and a saccade made to the target can curve towards an interesting distractor (Findlay & Harris, 1984; Van Gisbergen et al., 1987; Minken et al., 1993; Port & Wurtz, 2000; McPeek & Keller, 2001; McPeek et al., 2003). Curvature towards the distractor is the result of unresolved target-distractor competition and is directly related to the neural processing of object representations coded for both in the superior colliculus (SC) and frontal eye field (FEF) (McPeek et al., 2003; McPeek, 2006). Distractor neural activity increases above a baseline level causing curvature towards it in the subsequent saccade (McPeek & Keller, 2001; McPeek et al., 2003; Port and Wurtz, 2003). With enough time between stimulus onset and saccade initiation, the target-distractor competition can be fully resolved, and the neural activity encoding the distractor is suppressed below baseline causing saccades to curve away from the distractor (Doyle & Walker, 2001, 2002; McSorley et al., 2004; White et al., 2012). Thus, saccadic reaction time (SRT) plays a large role in saccade trajectories during target selection; shorter SRTs result in curvature towards the distractor and longer SRTs result in curvature away from the distractor (Theeuwes & Godijn, 2004; Walker et al., 2006; McSorley et al., 2006; Mulckhuyse et al., 2009; Hickey & van Zoest, 2012).

The common features or similarity between competing objects can also affect the amplitude of saccade curvature in a target selection task. The similarity between the target and distractor is an example of behavioural relevance, how bottom-up and top-down features come together to create priority rather than solely salience. Many studies have investigated the effect

of similarity on saccade trajectories by varying low level features such as colour and orientation. For example, previous studies have shown that there is more curvature towards a distractor that is colour congruent to the target than to a distractor that is colour incongruent (Ludwig & Gilchrist, 2003; Mulckhuyse et al., 2009). To examine the effects of similarity on saccade curvature for higher order objects rather than lower order feature singletons, Kehoe et al. (2018a) examined how the similarity between complex objects affects saccade curvature. They found that similarity and saccade curvature followed a linear relationship, where more saccade curvature was seen as there was less similarity between objects. They suggested the oculomotor system reweights the object representations coding the saccade goals, putting the most weight on the most behaviourally relevant object based on its features and similarity. The integration of the object representations and cortically processed visual information influences the final decision for the outputted saccade.

Most studies that have investigated the distractor's effect on saccade trajectories have kept the distractor at a set distance to the target as well as at a given similarity. Often the distractor identity is treated as a placeholder for a location to generate a competing motor plan (Sheliga et al., 1995) without any consequence to its identity. To understand the interplay of spatial distance and similarity, and the effects they have on saccade trajectories, we varied the distance and similarity between a target and distractor. Both the target and distractor objects were placed at isoeccentric points around a circle centred at fixation but varying in angular distance (AD), as encoded in an egocentric reference frame. This ensured the saccades made to either object were of the same length in order to compare the effects of target-distractor distance on saccade curvature metrics.

When varying the spatial layout of the objects, it is important to consider the attentional window around the target and the suppressive surround. Depending on the AD, and assuming there is enough time to suppress the distractor, the distractor could fall within the attentional window, within the suppressive surround, or outside of the suppressive surround (Desimone & Duncan, 1995). Spatial suppressive surrounds have been shown to follow a Difference of Gaussian (DoG) pattern, as predicted by the Selective Tuning model of visual attention (Tsotsos, 1990; Tsotsos et al., 1995; Cutzu & Tsotsos, 2003; Hopf et al., 2006). When the target and distractor are close, they are both in the attentional or excitatory spotlight, centered around the attended target. When the distractor object moves further away from the target, it is suppressed according to a gradient, where there is the most suppression at a medium distance, caused by pruning connections irrelevant to the stimulus-of-interest (Cutzu & Tsotsos, 2003; Yoo et al., 2018). Suppression is reduced at further distances until it disappears outside of the range of the attentional suppressive surround.

Suppressive surrounds have been found in feature-space for basic features such as colour, orientation, and direction of motion (Tsotsos et al., 2005; Tombu & Tsotsos, 2008; Störmer & Alvarez, 2014; Yoo et al. 2018). For example, Tombu and Tsotsos (2008) showed that as the distractor shifts further away from the target in feature space with regards to object orientation, attention follows a gradient suppressive surround pattern with the most suppression for closer orientations, and less for farther orientations. The feature-based suppressive surround has been examined for low order features, consistent with pruning neurons selective to similar features in feature-space in areas known to process those features, e.g. color in V4 (Zeki, 1973) or motion in the middle temporal area (Tootell et al., 1995; Huk et al., 2001). To extend this work, we are

interested in determining if a suppressive surround exists when attending to higher order, complex objects such as those used in our study.

In the present study, we investigated spatial layout, similarity, the interplay between them, and how their effects on saccade trajectory relate to spatial and object-based suppressive surrounds. After a temporal analysis of saccade direction over the period of target-distractor onset to saccade initiation, we split the saccade trajectory data for our subsequent analyses by SRT to directly examine the effects of time on the target-distractor competition process. We hypothesized that with enough time for this competition to resolve, as angular distance increases the distractor would be suppressed according to a spatial suppressive surround and would have a DoG-shaped effect on our saccade metrics. When varying the target-distractor similarity, we expected that if an object-based suppressive surround exists, we would find a similar DoG modulation of saccade trajectory shape. We expected that similarity would not be independent of angular distance effects since similarity computations are dependent on the local neural circuitry of the given visual area, which would be restricted by distance. Therefore, we hypothesized that if the angular distance and similarity effects interact, angular distance would induce a multiplicative gain effect on the effects of similarity on saccade trajectories.

4.4 Methods

4.4.1 Participants

Twenty-six participants recruited at York University (18-43 years old, 6 male) took part in this experiment, all with normal or corrected-to-normal vision. Participants were naïve to the purpose of the experiment and received partial course credit for participating, when applicable. They provided written informed consent prior to beginning the experiment. York University's Human Participants Review Committee approved this study.

4.4.2 Stimuli

The stimuli used were developed in-house using MATLAB (Mathworks, Natick, MA) and were based on an earlier study (Kehoe et al., 2018a). They consisted of a combination of 6 or 7 vertical and horizontal line segments (1° × 0.8°) positioned orthogonal to each other. This number of line segments was used to ensure holistic representations of the objects are used rather than depending on human visual working memory capacity (Luck & Vogel, 1997, Kehoe et al., 2018a). These stimuli were created to be novel to participants, and thus do not include letters or numbers in the English language. Line segments were white on a black background (white: CIExy [0.29, 0.30], luminance 126.02 cd/m^2, black: CIExy [0.27, 0.26], luminance 0.20 cd/m^2) and were put together to fit within a 2° × 2° box. Two sets of stimuli were used and shuffled throughout the experiment (Figure 4.1).

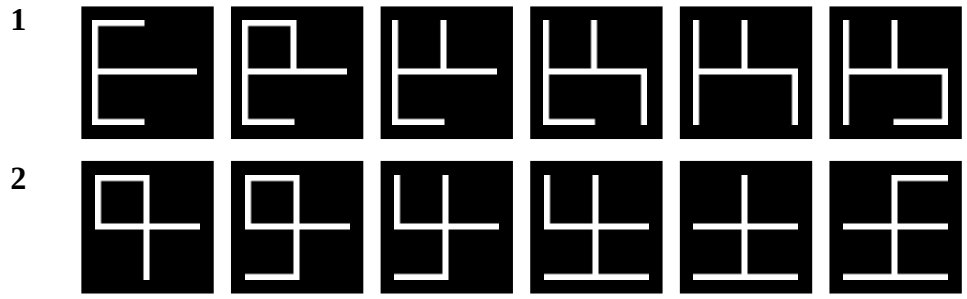

Figure 4.1: Stimulus sets 1 and 2. The stimuli were numbered from 1-6 (left to right). The difference between stimulus number gives rise to the number of line differences (objective similarity levels).

4.4.3 Apparatus

Experimental control was maintained with Presentation software (Neurobehavioral Systems, Berkeley, CA). Participants ran the experiment in a dark room on a 21-in CRT monitor (60Hz, 1024×768), 57cm away from a head and chin rest. Eye position was recorded from the left eye using an infrared eyetracker (500Hz; EyeLink II: SR Research, Ontario, Canada). Eye

position was calibrated at the start of the experiment and during the experiment, as necessary. Participants responded via a serial response box (Cedrus, San Pedro, CA; 6 participants) or mouse (Dell; 20 participants).

4.4.4 Procedure

The task was a delayed match to sample task where participants needed to search for a previously shown target object amongst a distractor object after a short delay from target preview. Participants started each trial when shown a small, white fixation cross (0.4° × 0.4°) at the centre of the screen by pressing a button (serial response box: center button; mouse: left button). The target object was then previewed on the screen (Figure 4.2A). Once ready, the participants pressed the button again, which replaced the preview with a central fixation cross. After fixating the cross for 200ms, the target and distractor objects appeared simultaneously at isoeccentric points around a circle of radius 8 dva. Participants were instructed to use their peripheral vision to identify the target while maintaining central fixation and respond by moving their gaze to the target. The trial ended when an eye movement was made within a 1.9 dva square box around the target or distractor, or after 750ms if no movement had been made. These time-out trials were reshuffled back into the remaining trial array. An error tone and message were used to indicate incorrect or time-out trials.

The target and distractor were placed at any of 16 equally spaced positions around the circle (Figure 4.2B). The target was randomly placed at one location and the distractor was placed relative to the target on either the clockwise or counterclockwise side. Similarity and AD between the target and distractor were varied and randomized for each trial. Lone target trials without a distractor were considered baseline trials and composed 20% of the total. This resulted in 50 trials per block, with 10 blocks for a total of 500 trials. Participants were given 10 practice

trials before block 1 which were not included in analysis. The experiment took ~45mins to complete. All participants included in the analysis completed the full 500 trials.

4.4.5 Similarity and angular distance

Objective similarity (OS) was determined by the amount of line segment differences between two given stimuli, defined by adding or removing individual line segments (Figure 4.1). Target-similarity differences were confined to the range OS 1-4. Angular distance (AD) was calculated as the absolute difference between target and distractor locations in polar angle (Figure 4.2B, C). AD range of ±1-5 was used in this experiment (Figure 4.2C).

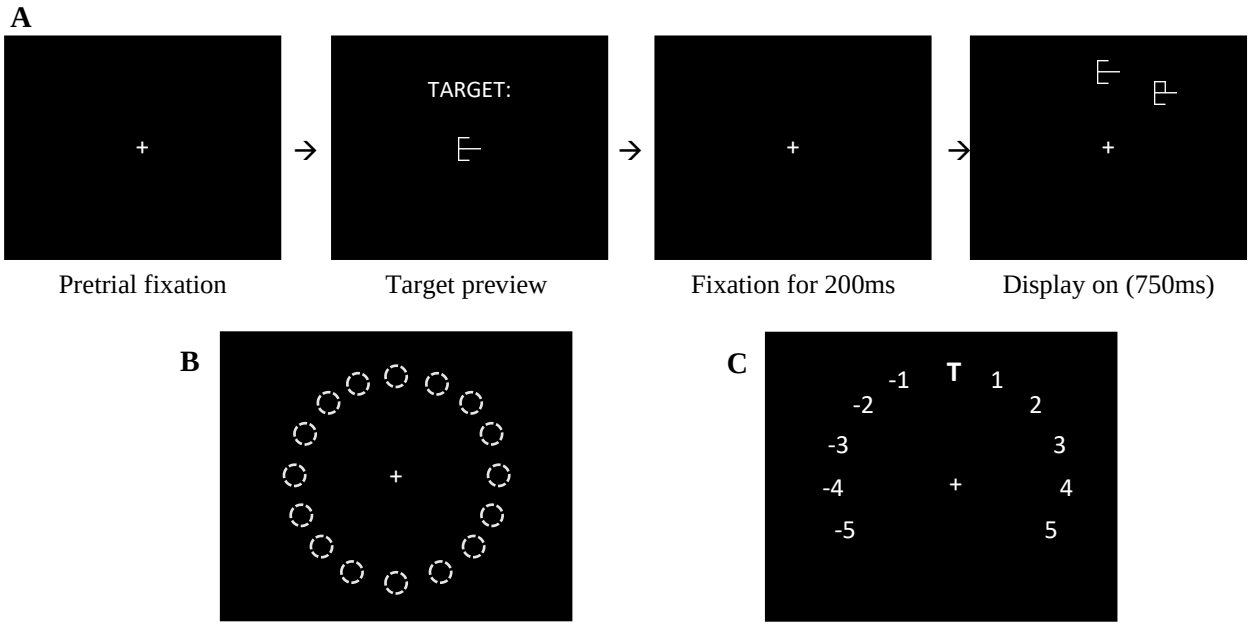

Figure 4.2. Task paradigm and display layout. *A:* Task paradigm. Participants fixated on the central cross and pressed a button to move to the target preview. Once ready, they pressed the button again to start the search. Participants stabilized fixation for 200ms then the display came on. The target and distractor remained visible until the participant fixated on an object or until 750ms had passed. *B:* 16 possible object locations, 22.5° apart, eccentricity of 8 dva. The target was randomly placed at one location and the distractor was placed relative to the target on the clockwise or counterclockwise side. *C:* AD locations relative to the target. With the target (T) at the top location as an example, the distractor could be placed from 1-5 positions clockwise, or 1-5 positions counterclockwise.

4.4.6 Analysis

4.4.6.1 Task performance: A binomial test was done on behavioural accuracy scores for each participant. No participants were excluded from analysis since all scores were significantly better than chance (50%).

4.4.6.2 Saccade detection: In-house written MATLAB scripts were used to filter saccades for each trial. We defined saccades as having a peak velocity over 50°/s, and for at least 8ms, a velocity that exceeded 20°/s. Only correct saccades in which the participants made a saccade to the target were included for analysis. The first saccade of each trial was analyzed and trials in which corrective saccades were needed to reach the target or blinks occurred were excluded from analysis. Saccades with an amplitude < 1° (1.26%) or with an SRT < 100ms (2.96%) were also excluded. In total, 16.18% of correct saccades were excluded from analysis.

4.4.6.3 Saccade metric calculations: Five saccade metrics were calculated for each saccade included in the analysis: initial angle, endpoint deviation angle, sum curvature, max curvature, and angle at max curvature. For all saccade metric calculations, the starting position of the saccade was shifted to the origin and rotated so the target position was on the positive y-axis at 8 dva. Initial angle was calculated as the angle between the line from the start of the saccade to the target, i.e. the y-axis, and the point 20% along the saccade trajectory. Endpoint deviation was calculated as the angular difference between the last point of the saccade trajectory and target, i.e. the y-axis. The curvature metrics were calculated with the saccade rotated so that both the start and end points lied on the positive y-axis. Sum curvature was calculated as the sum of all x-values from the points along the saccade trajectory. Max curvature was the x-coordinate value of the point with the maximum absolute x-value along the saccade trajectory. Angle at max curvature was the angular difference between a straight saccade, i.e. the y-axis, and the max

curvature coordinate. These metrics were baseline-subtracted using the average lone target trial metrics at the corresponding target location of that trial. Saccade metrics calculated from trials with negative ADs (counterclockwise placement of distractor relative to target) were reflected and collapsed with the clockwise distractors' positive AD metrics. This kept the distractor on the positive x side of the y-axis and resulted in 5 total ADs for analysis. All positive metrics signify deviations towards the distractor, and negative metrics signify deviations away from the distractor.

4.4.6.4 Average saccade trajectories: Average saccade trajectories were calculated and plotted using prior published techniques (Moehler & Fiehler, 2017). The x,y coordinates of saccades were separated by OS and/or AD and averaged together by first shifting the trajectory so that the first point was at the origin, and then taking points within 10% sections of the trajectory. Those points were averaged together to create an average saccade to visualize the calculated metrics. We baseline-corrected the x-coordinates of the trajectories by subtracting the values from the average lone target trial trajectory. Shaded regions around each average trajectory are SEM.

4.4.6.5 Metric plots and curve fits: Averages of the five metrics were plotted across the four OS levels and five ADs. Standard error of the mean (SEM) was calculated and plotted as error bars. We fit each plot with linear, quadratic, sigmoid, Gaussian, DoG, and exponential curves. We assessed the goodness of fit using the coefficient of determination (R^2), Akaike information criterion (AIC), and the p-value associated with the F-test of the regression analysis. In the range of ADs for our study, after reflecting and collapsing the clockwise (+AD) and counterclockwise (-AD) conditions together, a Gaussian fit was used to represent a DoG effect with respect to suppressive surrounds. Our experimental setup did not justify the use of a DoG

curve fit since we did not have the full range of data to represent the excitatory peak of a DoG curve that would occur between our +AD and -AD conditions. Thus, the single Gaussian was used to model the suppressive effect over collapsed ADs. Data was also split by OS across ADs to determine the effect of OS at each AD. For each metric, a 5 AD x 4 OS univariate ANOVA was performed in SPSS (v27, IBM) for short and long SRTs separately. Scheffe post-hoc analysis was used to investigate significant effects across conditions.

4.5 Results

4.5.1 Saccade target onset asynchrony and split saccadic reaction times

Saccade frequency, trial accuracy, and all five metrics were plotted across averaged saccade target onset asynchrony (STOA) values. STOA was calculated as the time between saccade initiation and target onset, where saccade initiation was taken to be at 0ms. STOA values were averaged over a sliding window of 10ms from -500 to -100ms. Each point plotted was an average of the metric data from trials with saccadic reaction times (SRTs) that fell within the sliding 10ms window. Trials with SRTs greater than 500ms (2.5% of total trials) were treated as outliers that were not representative of the rest of the data and were not included in analysis. Plotting saccadic frequency over STOA showed the peak frequency occurred at ~150ms, as would be expected with visually evoked saccades (Figure 4.3A). After this peak, there was a general decrease in saccade frequency. Accuracy over STOA (plotted as the percentage of trials that participants made a saccade to the target out of all total trails) showed that participants were more accurate the longer they took to process the display, as reflected in the STOA (Figure 4.3B). There was also more variance in accuracy at long SRTs. Since we split our subsequent analyses by short and long SRTs, it is important to note that trials with short SRTs made up 55%

of total trials included in analysis, whereas trials with long SRTs made up 30%. Only correct trials were included in analysis, where the participants made a saccade to the target.

Figure 4.3C showed that significant positive deviations towards the distractor occurred for short SRTs, and significant negative deviations away from the distractor occurred for long SRTs. The SRT range that fell in the middle was not significantly different than zero for each metric. This 'transition period' indicated the range of time where the process flipped from positive to negative deviations. The metrics were ordered by midpoint of the transition period from earliest to latest (Figure 4.3C). The curvature metrics reached the midpoint earlier than the angle metrics. All subsequent analyses were split for short and long SRTs outside of the transition period. For each analysis split by metric, the inclusive, metric-specific short and long SRT ranges were used, and the transition period was removed from analysis (see Table 4.1). The maximum spanning short and long SRT metric ranges were chosen as the ranges for the average saccade analysis. This analysis did not require data to be split by metric, so ranges were used to include the most data. Additionally, the metric data from trials with SRTs within the transition periods specific to each metric were plotted as histograms. Each metric histogram fit well with a single Gaussian distribution compared to a dual Gaussian, all with $R^2 > 0.96$ and $p < 0.001$.

Table 4.1. Short, transition period, and long SRT ranges (ms) for each metric and the average saccade analysis.

	Short SRT range	Transition period range	Long SRT range
Initial angle	100-228	230-260	262-500
Endpoint deviation	100-218	220-280	282-500
Sum curvature	100-216	218-250	252-500
Max curvature	100-214	216-250	252-500
Angle at max curvature	100-214	216-262	264-500
Average saccades	100-228	230-250	252-500

SRT, saccadic reaction time.

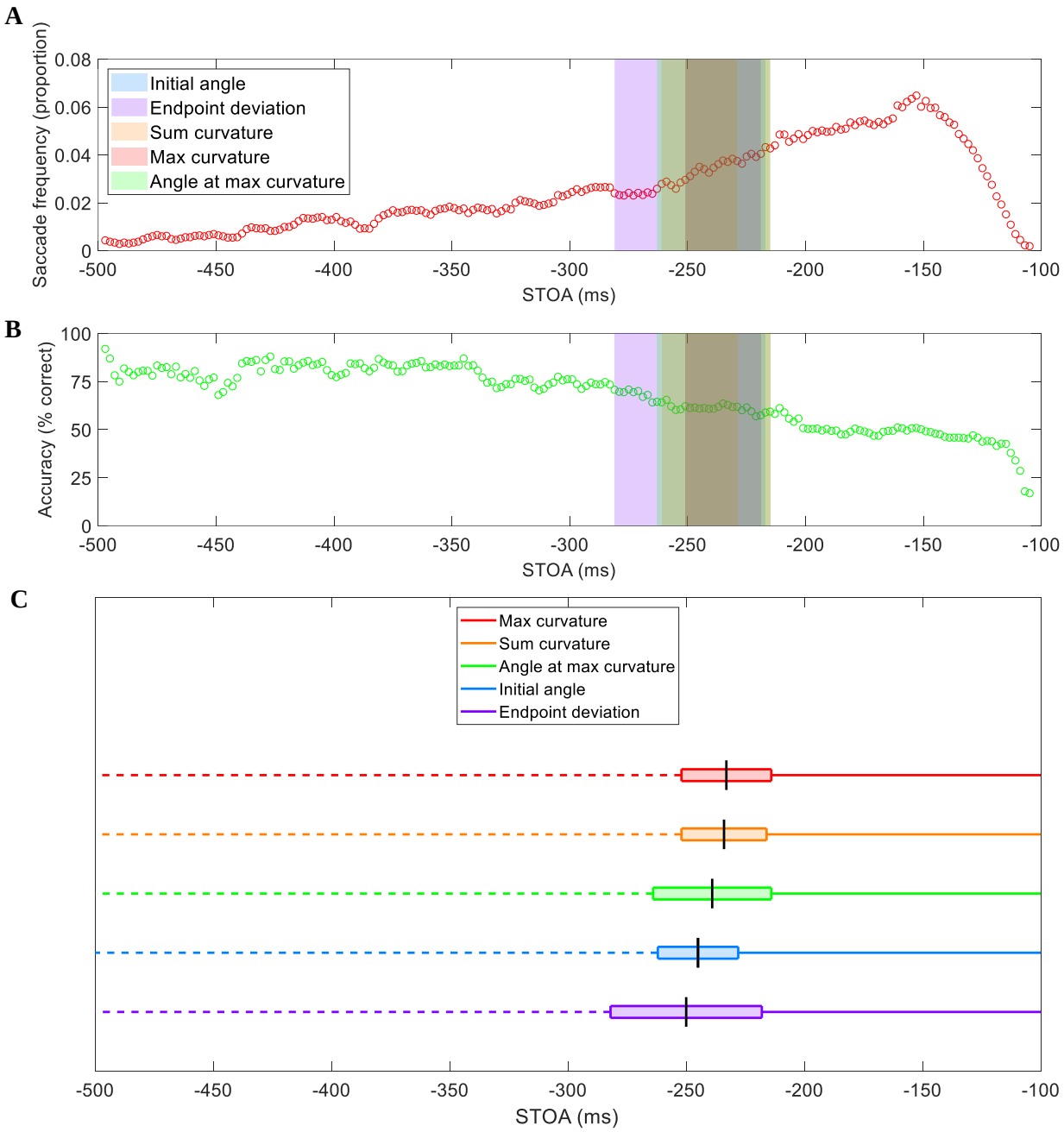

Figure 4.3. Saccade frequency, accuracy, and metrics over time. Shaded coloured regions cover the middle saccadic reaction time (SRT) period (transition period) for each metric that was removed from analysis. *A:* Saccade frequency plotted over STOA as a proportion of total trials. *B:* Accuracy plotted over STOA as a percentage of total trials. *C:* Transition period ranges by metric over SRT, ordered by midpoint from earliest to latest. The transition period is represented by the box and the midpoint is shown with a black vertical line. Each solid-coloured line represents the short SRT period where that metric significantly deviated towards the distractor. Each dashed-coloured line represents the long SRT period where that metric significantly deviated away from the distractor.

4.5.2 Average saccades

Average saccade trajectories were plotted across angular distance (AD) and objective similarity (OS) for short and long SRTs (Figure 4.4). The average saccades clearly depicted the effects SRT had on saccade deviation direction. We saw that saccades deviated positively for short SRTs versus negatively for long SRTs. When looking at the differences between OS levels and ADs, it is clear that AD had a greater effect on saccade trajectory compared to OS for short SRTs. Figure 4.4A showed a clear distinction between the average trajectories for AD = 1, 2 compared to AD = 3, 4, 5 in the initial angle and amount of curvature, all pointing towards the distractor. On the other hand, Figure 4.4B showed that the average trajectories for each OS were clustered together suggesting a lack of significant differences from each other. This was especially evident through the overlapping SEM shaded zones. For AD/long SRTs, Figure 4.4C showed evidence of a spatial suppressive surround; the average saccade trajectories for AD = 2, 3 were separated from those of AD = 1, 4, 5, and pointed more away from the distractor in initial angle and curvature. For OS/long SRTs, Figure 4.4D showed that the average saccade trajectories were more spread out between each OS, especially compared to those at short SRTs (Figure 4.4B).

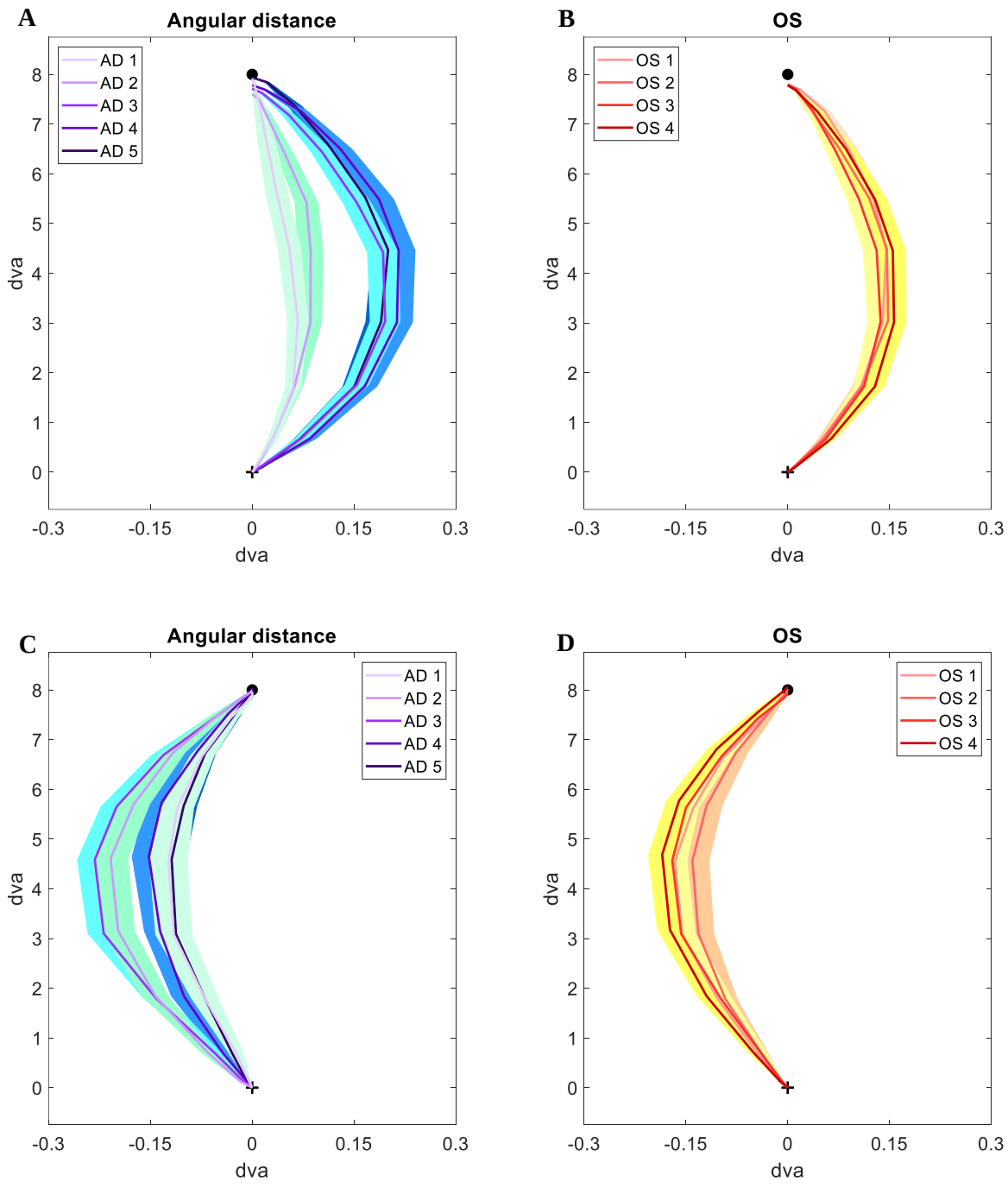

Figure 4.4. Average saccade plots for short and long SRTs split by objective similarity (OS) and angular distance (AD). Shaded regions represent the SEM for each average point along the trajectories. The black circle represents the target position at 8 dva. *A:* Average saccades for each AD for short SRTs. *B:* Average saccades for each OS for short SRTs. *C:* Average saccades for each AD for long SRTs. *D:* Average saccades for each OS for long SRTs.

4.5.3 Metrics over angular distance

The average metric values were split by short and long SRTs and plotted against AD (Figure 4.5A, B). Two-way ANOVAs for each metric across short SRTs showed main effects of AD on all metrics (initial angle $p < 0.001$, endpoint deviation $p < 0.001$, sum curvature $p < 0.001$, max curvature $p < 0.001$, angle at max curvature $p < 0.001$) (see Table 4.2). Scheffe post-hoc analysis for AD vs metrics for short SRTs showed: initial angle for AD = 1 was significantly different than ADs = 4, 5 ($p < 0.001$, $p = 0.002$), and AD = 2 was significantly different than ADs = 4, 5 ($p < 0.001$, $p = 0.003$); endpoint deviation for AD = 1 was significantly different than ADs = 3, 4, 5 (all $p < 0.001$), AD = 2 was significantly different than ADs = 3, 4, 5 (all $p < 0.001$), and AD = 3 was significantly different than ADs = 4, 5 ($p = 0.030$, $p = 0.002$); sum curvature for AD = 1 was significantly different than ADs = 3, 4, 5 (all $p < 0.001$), and AD = 2 was significantly different than AD = 3 ($p = 0.008$); max curvature for AD = 1 was significantly different than ADs = 3, 4, 5 (all $p < 0.001$), and AD = 2 was significantly different than AD = 3 ($p = 0.007$); angle at max curvature for AD = 1 was significantly different than ADs = 2, 3, 4, 5 ($p = 0.019$, rest $p < 0.001$), and AD = 2 was significantly different than ADs = 3, 5 ($p = 0.032$, $p = 008$).

For long SRTs, there were main effects of AD on all metrics (initial angle $p < 0.001$, endpoint deviation $p < 0.001$), sum curvature $p = 0.001$, max curvature $p < 0.001$, angle at max curvature $p = 0.020$ (See Table 4.2). Scheffe post-hoc analysis for AD vs metrics for long SRTs showed: initial angle for AD = 1 was significantly different than ADs = 2, 3 ($p = 0.23$, $p = 0.002$), and AD = 3 was significantly different than AD = 5 ($p = 0.025$); endpoint deviation for AD = 1 was significantly different than ADs = 2, 3, 4, 5 (all $p < 0.001$); sum curvature for AD = 1 was significantly different than ADs = 2, 3 ($p = 0.023$, 0.024); max curvature for AD = 1 was

significantly different than ADs = 2, 3 ($p = 0.009$, $p = 0.011$), AD = 2 was significantly different than AD = 5 ($p = 0.025$), and AD = 3 was significantly different than AD = 5 ($p = 0.029$). There were no significant differences across ADs for angle at max curvature.

We fit each metric plot with linear, quadratic, sigmoid, Gaussian, DoG, and exponential curves. We used goodness of fit metrics (R^2, AIC, p-values) to determine the best fit for each plot (see Table 4.3). The best curve fits for the AD/short SRTs plots were as follows (Figure 4.5A): initial angle – linear ($R^2 = 0.86$, AIC -1.21, $p = 0.024$); endpoint deviation – Gaussian ($R^2 = 0.99$, AIC = -17.27, $p < 0.001$); sum curvature – sigmoid ($R^2 = 0.97$, AIC = -13.87, $p = 0.009$); max curvature – sigmoid ($R^2 = 0.96$, AIC = -35.92, $p = 0.012$); angle at max curvature – sigmoid ($R^2 = 0.97$, AIC = -10.24, $p = 0.009$). Those for AD/long SRTs (Figure 4.5B): initial angle – Gaussian ($R^2 = 0.90$, AIC = 0.75, $p = 0.012$); endpoint deviation – quadratic ($R^2 = 0.96$, AIC -10.64, $p = 0.041$); sum curvature – Gaussian ($R^2 = 0.81$, AIC = 15.45, $p = 0.013$); max curvature – Gaussian ($R^2 = 0.86$, AIC = -32.76, $p = 0.010$); angle at max curvature – Gaussian ($R^2 = 0.86$, AIC = -8.11, $p = 0.007$). Gaussian and quadratic curves fit all metrics similarly for long SRTs, excluding endpoint deviation, but there was no F-test significance for quadratic curves and Gaussian curves are more suited for modelling neural mechanisms.

The results for the metrics over AD/short SRTs suggest that there was not enough time to inhibit the distractor and resolve the target-distractor competition (Figure 4.5A). The saccade vector was the weighted average of the two object locations (seen with the decreasing pattern for initial angle and endpoint deviation), which then curved when the objects were far enough to compete for attention. The latter was clear from the increase-to-plateau pattern for the curvature metrics. For AD/long SRTs, the DoG-shaped curve seen for all metrics was indicative of the

spatial suppressive surround where there was the most suppression of the distractor and most curvature away at AD = 3 (Figure 4.5B).

4.5.4 Metrics over similarity

The average metric values were plotted against OS for short and long SRTs (Figure 4.6A, B). For short SRTs, there were no main effects of OS on the metrics. For long SRTs, there were main effects of OS on endpoint deviation ($p = 0.020$) (see Table 4.2), but there were no significant differences across OS levels according to Scheffe post-hoc analysis. There were no significant interaction effects between OS and AD for short or long SRTs.

A variety of curves were fit to the metrics plotted against OS. The best curve fits according to goodness of fit measures for OS/short SRTs (Figure 4.6A) were as follows: initial angle – linear ($R^2 = 0.76$, AIC = -10.92, $p = 0.127$); endpoint deviation – quadratic ($R^2 = 0.99$, AIC = -32.47, $p = 0.031$); sum curvature – quadratic ($R^2 = 0.24$, AIC = -13.34, $p = 0.874$); max curvature – quadratic ($R^2 = 0.92$, AIC = -44.39, $p = 0.287$); angle at max curvature – quadratic ($R^2 = 0.93$, AIC = -21.09, $p = 0.272$). For OS/long SRTs (Figure 4.6B): initial angle – quadratic ($R^2 = 0.99$, AIC = -15.13, $p = 0.084$); endpoint deviation – quadratic ($R^2 = 0.91$, AIC = -12.13, $p = 0.296$); sum curvature – quadratic ($R^2 = 0.64$, AIC = 11.53, $p = 0.604$); max curvature – quadratic ($R^2 = 0.47$, AIC = -33,52, $p = 0.729$); angle at max curvature – quadratic ($R^2 = 0.55$, AIC = -6.56, $p = 0.668$).

For OS/short SRTs, there were no significant effects of similarity on saccade trajectories, except for endpoint deviation (Figure 4.6A). The lack of effect from similarity was expected since at short SRTs there was not enough time to fully cortically process both objects and inhibit the distractor to resolve the target-distractor competition. The pattern found for endpoint deviation suggests that an object-based suppressive surround modulates endpoint deviation while

discriminating the objects. For OS/long SRTs, we saw a downwards sloping significant trend for initial angle ($p = 0.084$), showing that the saccades angled away from the distractor more when the objects were less similar to each other (Figure 4.6B).

Table 4.2. AD and OS main effect ANOVA p-values for each metric for short and long SRTs.

	Short SRTs		**Long SRTs**	
	AD	**OS**	**AD**	**OS**
Initial angle	**< 0.001***	0.606	**< 0.001***	0.052
Endpoint deviation	**< 0.001***	0.311	**< 0.001***	0.020*
Sum curvature	**< 0.001***	0.746	**0.001***	0.470
Max curvature	**< 0.001***	0.831	**< 0.001***	0.736
Angle at max curvature	**< 0.001***	0.658	0.020*	0.267

*p-value is significant ($p < 0.05$). Bolded entries highlight where Scheffe post-hoc analysis showed significant differences across conditions. AD, angular distance; OS, objective similarity; SRT, saccadic reaction time.

Table 4.3. R^2, AIC values for each curve fitted to metric plots over AD and OS for short and long SRTs.

Condition	SRT Period	Curve fit	Initial angle	Endpoint deviation	Sum curvature	Max curvature	Angle at max curvature
AD	Short	Linear	**0.86, -1.21**	0.91, 1.96	0.69, -4.55	0.67, -28.38	0.82, -3.27
		Quadratic	0.87, 0.46	0.94, -2.01	0.94, -10.57	0.94, -34.81	0.95, -7.43
		Sigmoid	0.87, 1.57	0.99, -15.42	**0.97, -13.87**	**0.96, -35.92**	**0.97, -10.24**
		Gaussian	0.86, 1.62	**0.99, -17.27**	0.91, -7.90	0.91, -31.90	0.88, -2.36
		DoG	0.90, 1.81	0.95, 1.78	0.94, -9.89	0.94, -34.24	0.96, -7.83
		Exponential	0.86, -0.52	0.88, 4.52	0.55, -2.03	0.54, -26.04	0.69, 0.10
	Long	Linear	0.01, 8.83	0.49, -0.05	0.00, -2.51	0.00, -25.93	0.14, -2.20
		Quadratic	0.90, -0.52	**0.96, -10.64**	0.81, -8.93	0.86, -33.77	0.82, -7.98
		Sigmoid	0.55, 10.52	0.91, -6.78	0.50, -1.95	0.44, -24.59	0.14, 1.62
		Gaussian	**0.90, 0.75**	0.77, -0.81	**0.81, 15.45**	**0.86, -32.76**	**0.86, -8.11**
		DoG	0.00, 10.39	0.91, -5.15	0.40, 0.14	0.00, -23.31	0.00, 7.64
		Exponential	0.01, 10.04	0.35, 2.25	0.00, -1.06	0.00, -24.56	0.13, -0.63
OS	Short	Linear	**0.76, -10.92**	0.14, -7.22	0.00, -14.27	0.00, -36.43	0.44, -14.99
		Quadratic	0.77, -9.00	**0.99, -32.47**	**0.24, -13.34**	**0.92, -44.39**	**0.93, -21.09**
		Sigmoid	0.76, -7.86	0.00, -5.25	0.00, -11.43	0.00, -32.68	0.46, -12.27
		Gaussian	0.76, -7.91	0.15, -4.40	0.00, -11.51	0.00, -33.62	0.45, -12.20
		DoG	0.73, -7.74	0.31, -4.95	0.00, -11.55	0.00, -32.41	0.48, -12.27
		Exponential	0.77, -10.19	0.15, -6.40	0.00, -13.60	0.00, -35.34	0.46, -14.21
	Long	Linear	0.96, -10.03	0.85, -12.03	0.63, -13.44	0.21, -33.91	0.08, -5.67
		Quadratic	**0.99, -15.13**	**0.91, -12.13**	**0.64, -11.53**	**0.47, -33.52**	**0.55, -6.56**
		Sigmoid	0.98, -8.46	0.89, -10.50	0.63, -10.02	0.31, -30.98	0.23, -2.90
		Gaussian	0.97, -5.06	0.88, -10.18	0.64, -10.09	0.48, -4.95	0.57, -5.21
		DoG	0.86, -2.37	0.78, -7.73	0.65, -10.95	0.20, -30.53	0.02, -2.42
		Exponential	0.98, -11.57	0.89, -12.27	0.62, -12.50	0.20, -33.31	0.08, -5.12

Bolded entries highlight the best curve fit for the respective plot. AD, angular distance; OS, objective similarity; SRT, saccadic reaction time.

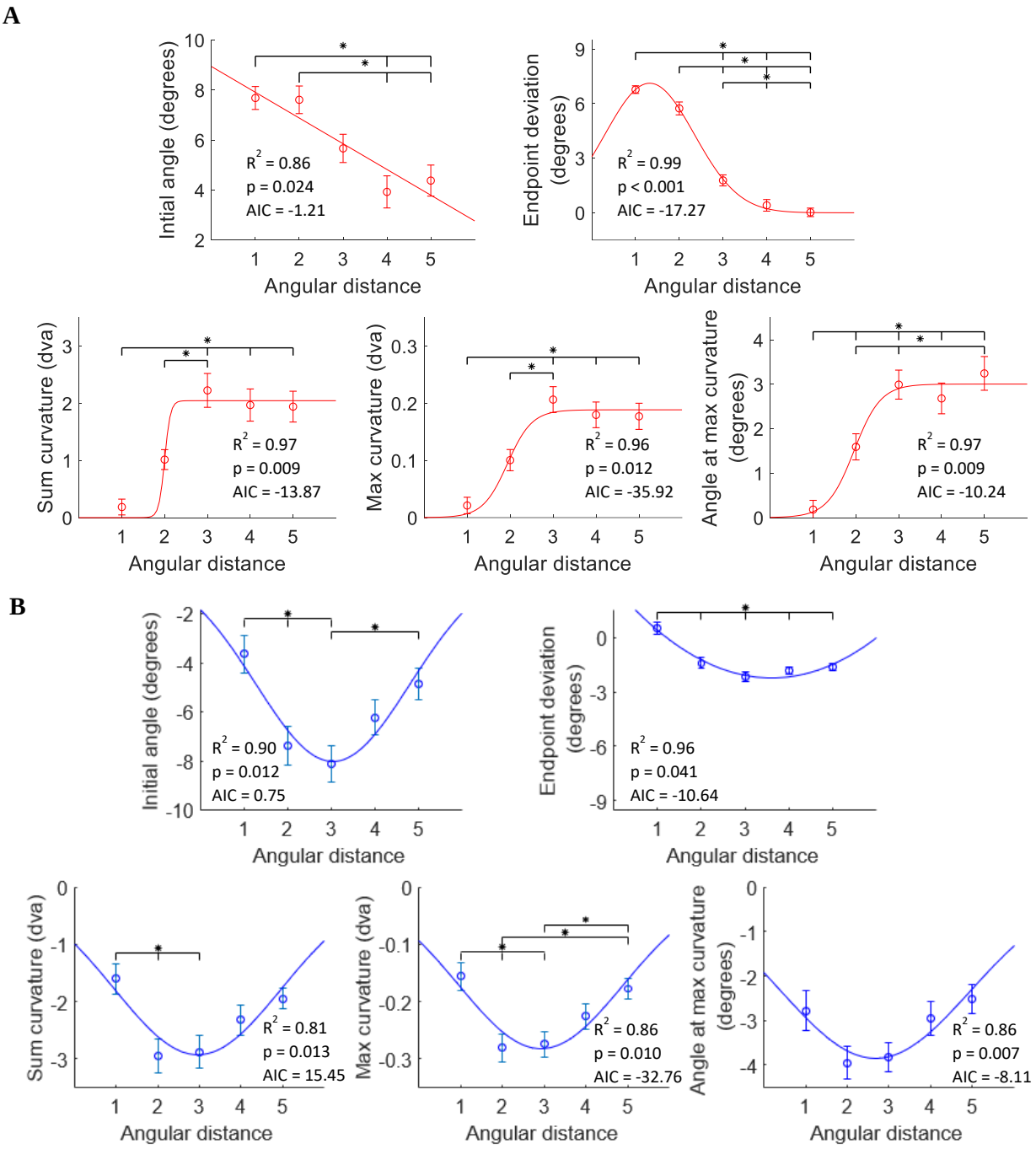

Figure 4.5. Saccade metric averages over angular distance (AD) with curve fits for short and long saccadic reaction times (SRTs). Curve fits were chosen according to goodness of fit metrics (R^2, AIC, p). Plots include the respective R^2, p-values, and AIC. Error bars are SEM. Brackets indicate significant differences ($p < 0.05$) from Scheffe post-hoc analysis. *A:* Metrics over AD for short SRTs. Curve fits from left to right: linear, sigmoid, sigmoid, sigmoid, Gaussian. *B:* Metrics over AD for long SRTs. Curve fits were all Gaussian except quadratic for endpoint deviation.

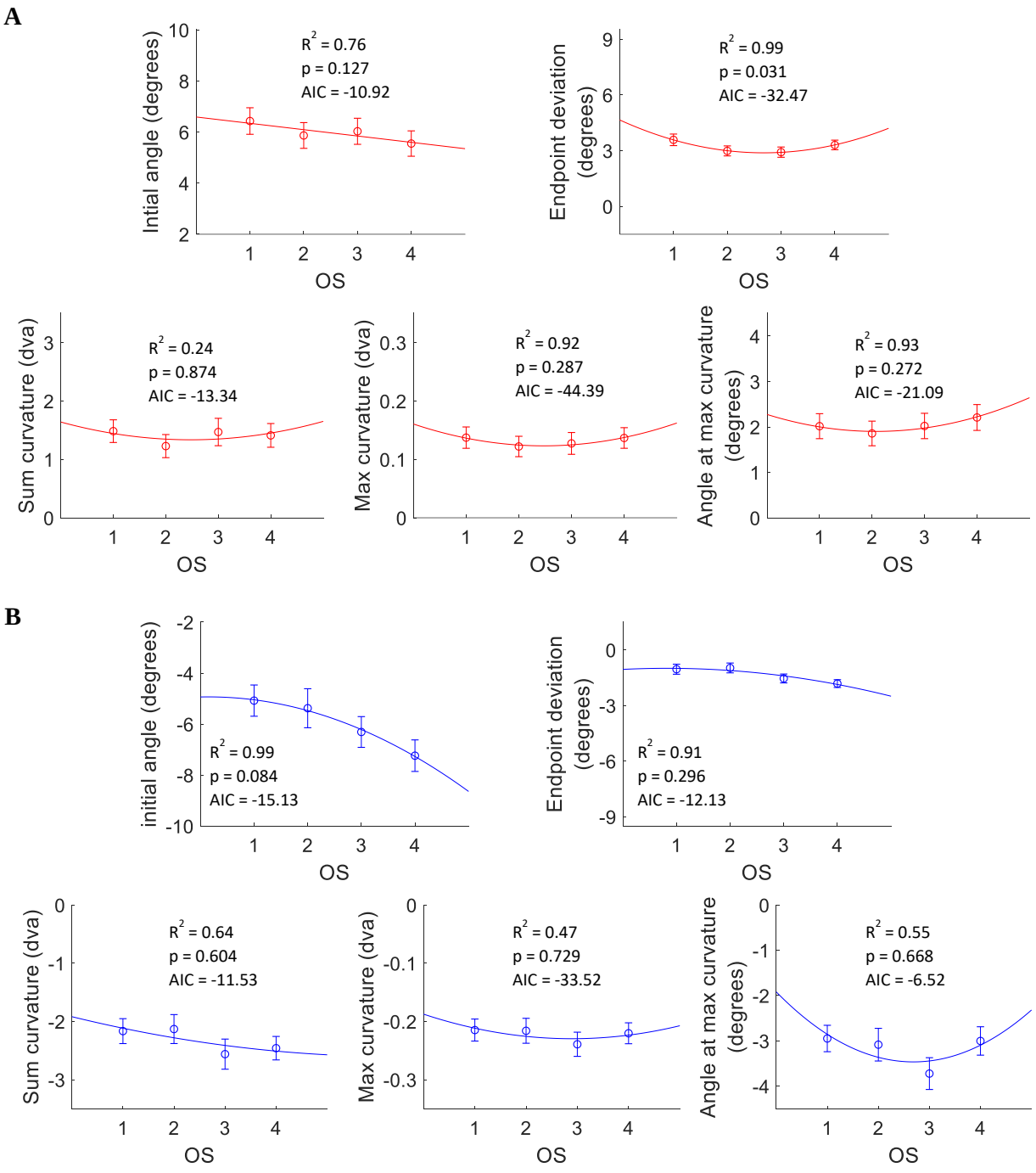

Figure 4.6. Saccade metric averages over objective similarity (OS) with curve fits for short and long saccadic reaction times (SRTs). Curve fits were chosen according to goodness of fit metrics (R^2, AIC, p). Plots include the respective R^2, p-values, and AIC. Error bars are SEM. *A:* Metrics over OS for short SRTs. Curve fits were all quadratic except linear for initial angle. *B:* Metrics over OS for long SRTs. Curve fits were all quadratic.

4.5.5 Similarity-angular distance split plots

To better investigate the relationship between OS level and AD, we plotted the average metric values across AD with separate lines for each OS level (Figure 4.7). The overall patterns match those of the averaged metric plots from Figure 4.5A, B. We fit each line with the best curve fits from Figure 4.5A, B for their respective SRT periods. For both short and long SRTs, the best fit of the average metric plots (see Table 4.4) matched well to the individual similarity lines with most curves showing significant trends ($p < 0.1$).

Table 4.4. R^2, AIC, p-values for each curve fitted to metric plots over AD separated by OS for short and long SRTs.

SRT Period	Metric (Curve fit)	OS 1	OS 2	OS 3	OS 4
Short	Initial angle (Linear)	**0.83, -2.01, 0.030**	0.09, 5.49, 0.626	0.44, 9.04, 0.220	0.89, -2.44, 0.459
	Endpoint deviation (Gaussian)	**0.99, 16.76, <0.001**	**0.987, 16.35, 0.009**	**0.99, 17.96, 0.009**	**0.99, 17.73, 0.002**
	Sum curvature (Sigmoid)	**0.83, -5.92, 0.041**	**0.97, -16.50, 0.009**	**0.72, 4.04, 0.031**	**0.91, -1.13, 0.004**
	Max curvature (Sigmoid)	**0.77, -28.85, 0.054**	**0.97, -41.14, 0.007**	**0.69, -22.23, 0.047**	**0.93, -32.28, 0.028**
	Angle at max curvature (Sigmoid)	**0.90, -8.91, 0.015**	**0.98, -12.29, 0.008**	**0.71, 8.07, 0.046**	**0.91, -2.20, 0.038**
Long	Initial angle (Gaussian)	**0.88, 18.55, 0.026**	**0.62, 9.47, 0.078**	**0.20, 8.21, 0.048**	**0.94, 0.57, 0.007**
	Endpoint deviation (Quadratic)	0.76, -0.92, 0.240	**0.97, -9.15, 0.031**	**0.96, -13.45, 0.037**	**0.92, -7.74, 0.080**
	Sum curvature (Gaussian)	**0.63, -4.22, 0.031**	**0.70, -2.89, 0.043**	**0.32, 2.54, 0.087**	**0.67, -4.06, 0.026**
	Max curvature (Gaussian)	**0.77, -30.34, 0.018**	**0.73, -27.56, 0.031**	**0.34, -21.21, 0.085**	**0.85, -32.20, 0.012**
	Angle at max curvature (Gaussian)	**0.64, -1.10, 0.031**	**0.51, -0.35, 0.035**	**0.23, 5.50, 0.074**	**0.94, -10.63, 0.004**

Bolded entries highlight significant effects ($p<0.05$) or significant trends ($p<0.1$). AD, angular distance; OS, objective similarity; SRT, saccadic reaction time.

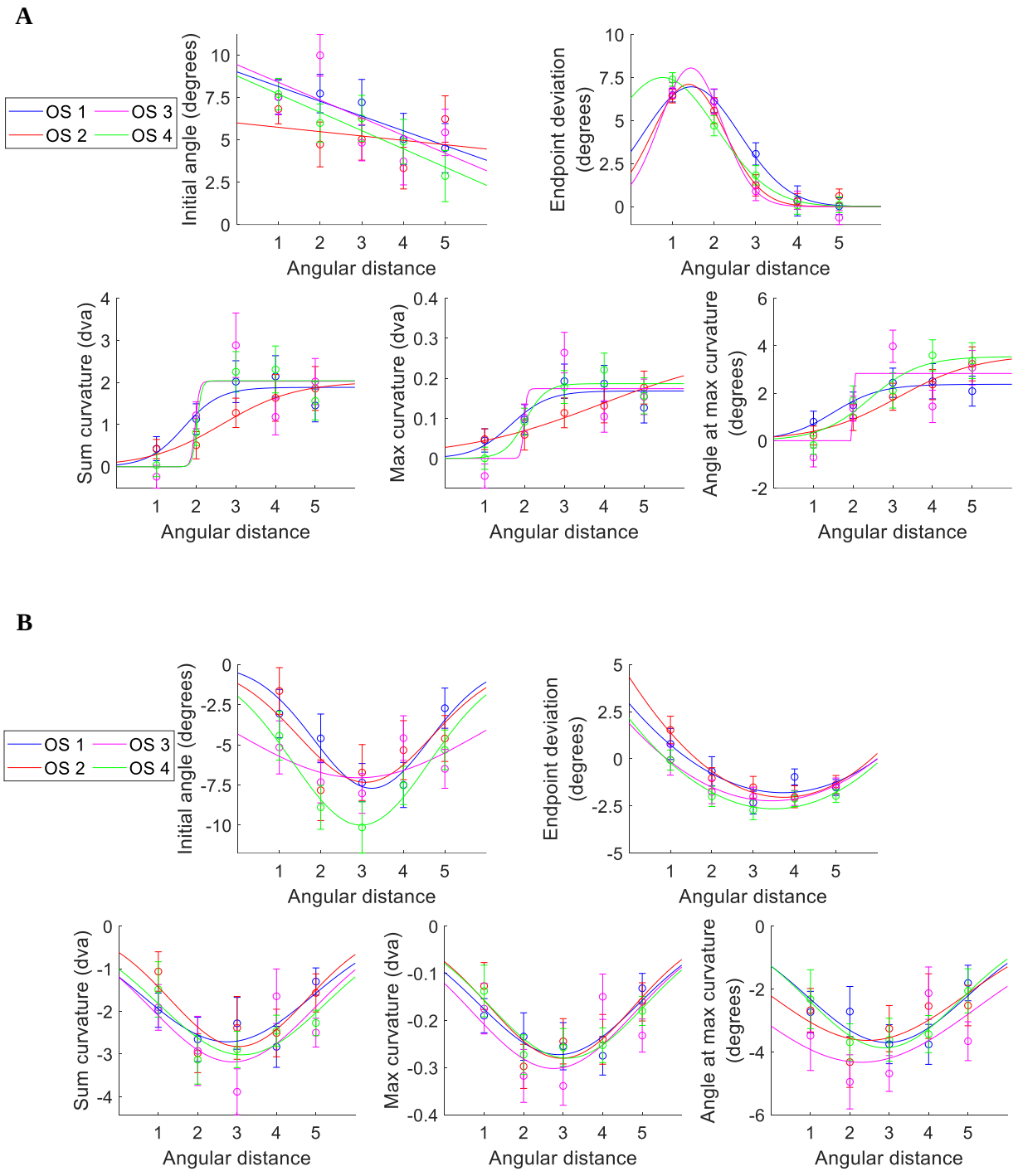

Figure 4.7. Metrics over angular distance (AD) with separate lines for objective similarity (OS) 1-4, plotted for short and long saccadic reaction times (SRTs). Each plot was fit with the respective best fit per metric from the average metric plots. *A:* Metrics over AD with split OS lines for short SRTs. *B:* Metrics over AD with split OS lines for long SRTs.

4.5.6 Gradient plots

We depicted the significant trends ($p < 0.1$) from the average metric plots (Figures 4.5 & 4.6) with radial gradient plots in distance (Figure 4.8) and object space (Figure 4.9). The darkest red and blue colours represent the most deviation towards and away from the distractor, respectively. The lighter the colour, the closer the metric was to no deviation. Figure 4.8A depicted the effects of AD on saccade metrics at short SRTs pointing towards the distractor, where initial angle and endpoint deviation showed a decreasing trend as distance increases, whereas the curvature metrics showed an increasing trend to a plateau at AD = 3. Figure 4.8B illustrated the effects of AD at long SRTs and showed a suppressive surround pattern for all metrics pointing away from the distractor, consistent with a DoG-shaped spatial suppressive zone. Figure 4.9A depicted the effects of OS on endpoint deviation for short SRTs as a suppressive surround in object space where there was less endpoint deviation towards the distractor at the middle similarity levels (OS = 2, 3). Figure 4.9B showed the effects of OS at long SRTs through a decreasing trend for initial angle, pointing more away from the distractor as OS increased.

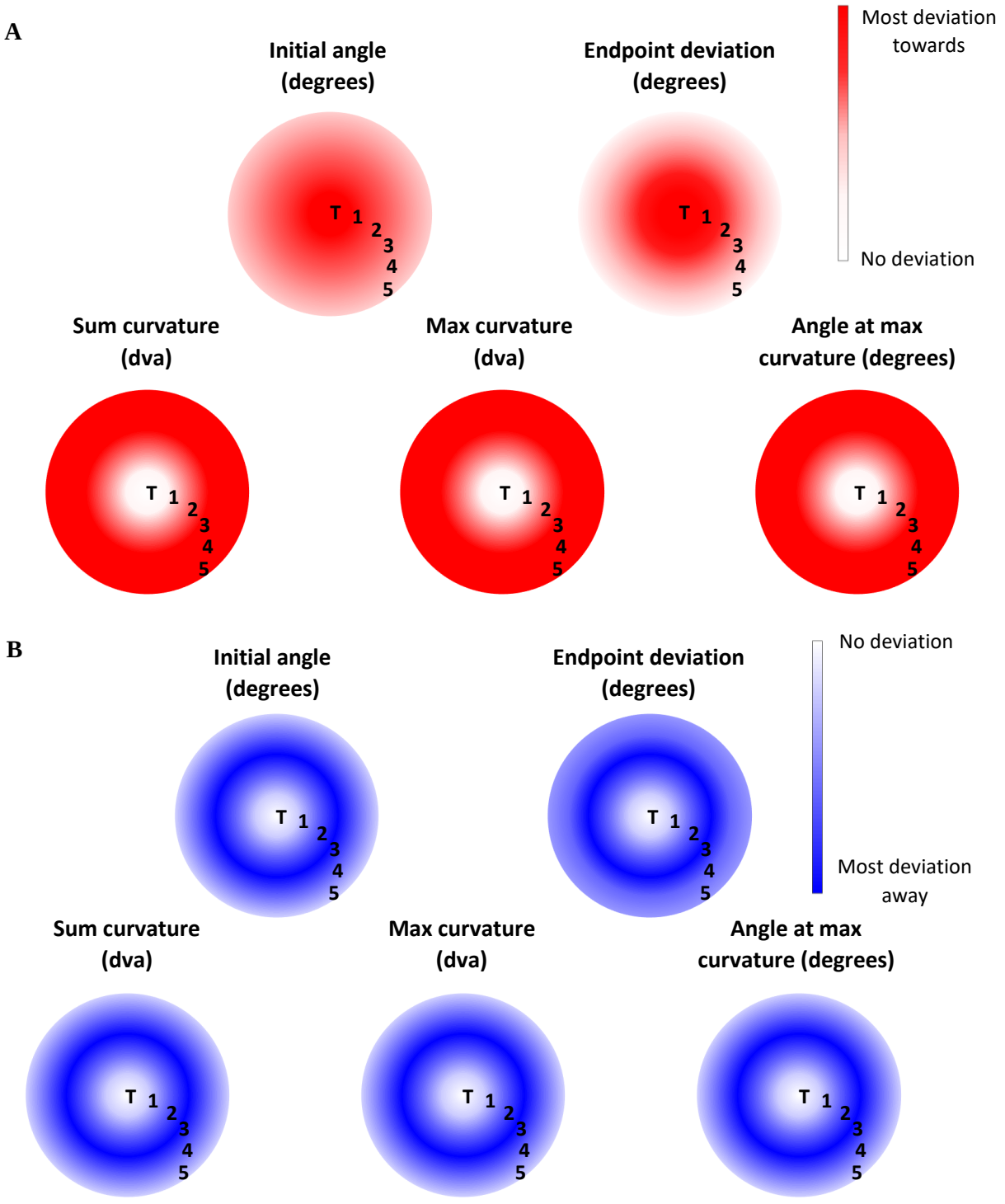

Figure 4.8. Metric plots depicted as radial gradients over angular distance (AD) for short and long saccadic reaction times (SRTs). Target and distractor positions in space are shown with T and AD 1-5. Darker colours represent the most deviation towards or away from the distractor. White represents no deviation. *A*: Gradient plots over AD for short SRTs. *B*: Gradient plots over AD for long SRTs.

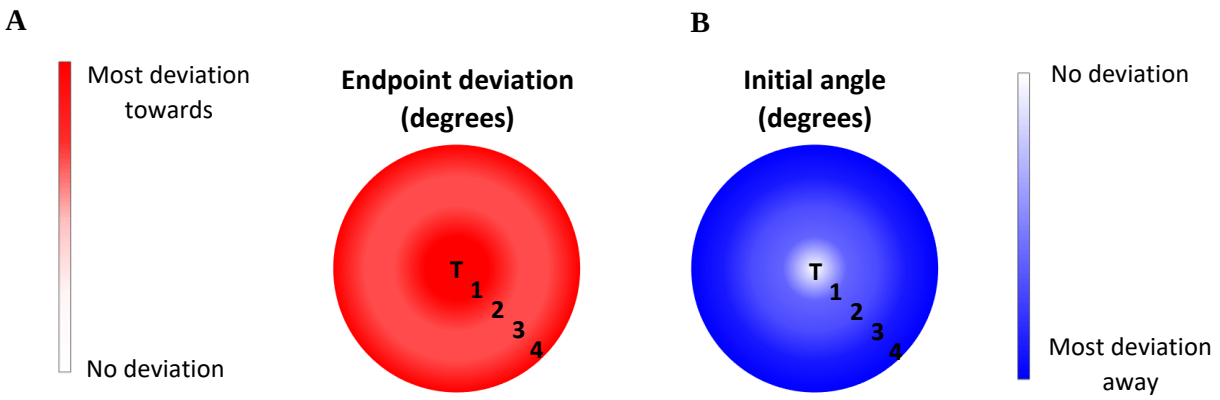

Figure 4.9. Metric plots depicted as radial gradients over objective similarity (OS) for short and long saccadic reaction times (SRTs). These depictions were created for significant trends ($p < 0.1$) which occurred for endpoint deviation and initial angle for OS/short SRTs and OS/long SRTs, respectively. Target and distractor positions in object space are shown with T and OS = 1-4. Darker colours represent the most deviation towards or away from the distractor. White represents no deviation. *A*: Gradient plot over OS for short SRTs. *B*: Gradient plot over OS for long SRTs.

4.6 Discussion

We examined the effects of varying the angular distance (AD) and similarity of complex target and distractor objects on the shape of saccade trajectories made to the target during a delayed match to sample task to elucidate how perceptual and spatial relationships are encoded by the oculomotor system. We aimed to relate these effects to spatial and object-space suppressive surrounds, as well as examine the interactions between the variables. The time between display onset and saccade initiation influenced saccade direction, prompting us to further analyze the effects of saccadic reaction time (SRT) on saccade metrics. While prior studies have generally shown differential effects of distractor attraction and inhibition based on timing, we determined the time course of these processes for each of the 5 saccade trajectory metrics. The effects of SRT on the saccade metrics reflects the development of the competition process between the two saccade goals; more time between target-distractor onset and saccade

initiation resulted in more time to resolve competition and inhibit the distractor object. When there was not enough time to resolve the competition between target and distractor, there was little effect of AD on saccade trajectories, consistent with saccade vector averaging and an incomplete winner-take-all (Port & Wurtz, 2003). With increasing SRT, AD modulated the saccade metrics, following the pattern of a spatial suppressive surround. On the other hand, varying the target-distractor similarity influenced endpoint deviation angle at short SRTs, suggesting an object-based suppressive surround exists during the discrimination phase of competition. At long SRTs, varying similarity affected initial angle linearly, showing saccades pointing more away from the distractor as the object similarity decreased. The following discussion will take an in depth look at our findings and their implications on the underlying neural circuitry and mechanisms involved in target selection processing.

4.6.1 Effects of saccadic reaction time on saccade direction

Our results regarding the effects of SRT on saccade trajectory direction (towards/away from the distractor) replicate previous findings in literature (McSorley et al., 2006; Walker et al., 2006). Although we did not purposefully manipulate the SRT period duration, the time participants took to decide which object was the target and initiate a saccade naturally varied across trials within the allotted 750ms. When participants took a short amount of time (short SRTs), the saccades curved towards the distractor; when participants took more time before saccade initiation (long SRTs), the saccades curved away from the distractor. This is dependent on the timing of the target-distractor competition process, or more specifically the time it takes to develop distractor inhibition and decrease the neural activity coding the saccade goal location below a baseline level. Our findings are consistent with previously found results that suggest distractor inhibition occurs after approximately 200-220ms from display onset (McSorley et al.,

2006). With a shorter SRT period (~100-220ms), the target-distractor competition remained unresolved by the time of saccade initiation, and the objects could not be fully cortically processed in time to allow for inhibition of the distractor. This resulted in curvature towards the distractor that was aimed more towards a weighted average vector location between the target and distractor objects. On the other hand, with a longer SRT period (~260-500ms), there was enough time to inhibit the distractor object causing saccades to curve away from the distractor on the way to the target. In the 'transition period' between what we categorized as short and long SRTs (~220ms-260ms), saccade deviation was in transition between being towards and away from the distractor.

Additionally, we found that each metric had a different transition period range. We ordered these ranges from earliest to latest by the midpoint of the transition period, which was an approximate time for when the metrics flipped from deviating towards to away. Our results showed that the curvature metrics (sum curvature, max curvature, and angle at max curvature) reached the midpoint earlier than the angle metrics (initial angle and endpoint deviation angle). This suggests that after competition resolves and the process flips to distractor inhibition, saccade curvature is affected sooner than initial angle and endpoint deviation. As well, all three curvature metrics reflect the residual effects of an incomplete winner-take-all process. Although they are not independent from each other, they have been used individually and in the aggregate in past studies. Similarly, initial angle and endpoint deviation can be grouped due to their involvement in saccade planning and consistency with weighted vector averaging. The ordering of transition period midpoints further supports this grouping. These findings for saccade angle and curvature are consistent with what has been shown for smooth pursuit eye movements. Recanzone & Wurtz (1999) demonstrated that the initial speed and direction of smooth pursuit to

a moving target amongst a distractor reflected weighted vector averaging. After more time, the process flipped to be more consistent with a winner-take-all process (Recanzone & Wurtz, 1999). The differences between our results for saccade angle and saccade curvature are reflective of the transition from weighted vector averaging to a winner-take-all model.

4.6.2 Effects of angular distance on saccade trajectories

For short SRTs, our results showed that initial angle and endpoint deviation decreased with increasing AD. These saccade angle metrics are reflective of weighted vector averaging of the saccade plans prior to movement initiation. Our results showed that the saccade angle was shifted more towards the target with increasing AD, suggesting that when planning a saccade to one location, competing plans increase in strength the closer they are to the intended saccade goal. A decreasing pattern was seen for both initial angle and endpoint deviation, supporting that the saccade's initial trajectory and endpoint location are related and separate from the curvature metrics in terms of saccade motor planning. This is consistent with findings in literature proposing the initial direction and endpoint deviation of a saccade are correlated (Van der Stigchel & Theeuwes, 2007), refuting other models that propose no relation between the two metrics since they postulate endpoint deviation should be influenced by the on-line correction bringing the saccade towards the target (McSorley et al., 2004).

The three curvature metrics showed evidence of an incomplete winter-take-all process between the locations of the target and distractor that developed from saccade goal competition. As AD increased, saccade curvature increased and then plateaued. This finding showed that increasing AD only affected saccade curvature up to a point where it remained at a maximum value from AD 3-5. This suggests that if AD were increased even further, saccade curvature would remain set at the maximum value, but the curvature must drop-off eventually. If the

distractor were placed directly underneath the target (AD = 180°), both saccade goals would no longer compete, and a saccade made to the target would be consistent with one made to a lone target on the display. Our results suggest the initial and endpoint deviation angles could be planned pre-movement, creating a saccade vector set at the weighted average location of the target and distractor. The pattern we observed for saccade curvature suggests that there is a maximum amount the distractor can pull in the saccade and therefore a maximum curvature. Overall, theses results showed the effects of varying AD on saccade trajectories when the target-distractor competition had not had enough time to resolve, since the saccades deviating towards the distractor were exclusively seen.

For long SRTs, initial angle and endpoint deviation angle metrics were modulated in a DoG-shaped curve away from the distractor as AD increased. The same DoG-shaped curves were also found for the curvature metrics. These findings provide evidence of a spatial suppressive surround in oculomotor planning as was predicted for visual processing by the Selective Tuning model of attention (Cutzu & Tsotsos, 2003; Hopf et al., 2006). When the distractor was close to the target (AD 1 and 2) it was in the attentional window of the target and less suppression was induced. When the distractor was at a medium distance from the target (AD 3), it was the most suppressed due to the gradient suppressive surround and the peak suppression at this location. Finally, as the distractor moved far enough away to be outside of the suppressive zone surrounding the attended target (AD 4 and 5), the distractor suppression was weaker and curvature away lessened. Neurophysiological evidence of a suppressive DoG gradient surrounding the attentional spotlight has been found in early and intermediate areas of the visual cortex (Müller & Kleinschmidt, 2004; Hopf et al., 2006), consistent with the selective tuning model (Tsotsos, 1990; Tsotsos et al., 1995) and the divisive normalization model (Reynolds &

Heeger, 2009). This spatial suppressive surround shown for attention in visual processing is reflected in saccade trajectories, which provides evidence that oculomotor planning is dependent on an attentional priority map with weighted representations of targets and distractors.

4.6.3 Effects of similarity on saccade trajectories

Once again, we split our similarity results into short and long SRTs to assess how similarity affects the competition phase separately from the distractor inhibition phase after the competition is resolved. For short SRTs, there were no statistically significant differences between similarity levels when examining the angle metrics over increasing OS (as the objects became less similar). Despite this finding, there was a significant DoG-shaped pattern for endpoint deviation angle. This is consistent with a suppressive surround as seen for simple, lower order features such as colour, orientation, and direction of motion (Tsotsos et al., 2005; Tombu & Tsotsos, 2008; Störmer & Alvarez, 2014; Yoo et al. 2018; Kehoe et al., 2018b). The distractor at OS 2 and 3 was suppressed compared to at OS 1 and 4; the endpoint deviation angle at OS 2 and 3 was pointing less towards the distractor compared to at OS 1 and 4. This suggests that an object-based suppressive surround is active during and effects the discrimination phase of target-distractor competition. When trying to search for the target object and resolve the competition between saccade goals, the suppressive surround inhibits the distractor in object space when it is at a medium similarity to the target. Therefore, the distractor has less of an effect on endpoint deviation at these similarity levels, causing the saccades to land closer to the target. Despite this pattern of inhibition, the overall effect of similarity at these short SRTs showed saccades pointing in the positive, towards direction, suggesting the distractor had not been fully suppressed before saccade initiation. Therefore, computing the target-distractor similarity

enough to completely inhibit the distractor may take a longer time compared to processing the distance between them.

For long SRTs, we saw evidence of more complete distractor inhibition from the overall negative deviations seen for each metric. When the target and distractor were less similar, the initial angle was better directed away from the distractor. It is easier to suppress an object more different from its competitor (Perry & Fallah, 2014), which was reflected in the decreasing trend of initial angle as OS increased. There were no effects of similarity on saccade curvature during the late phase of competition. As well, the lack of a DoG-shaped effect from any metric at long SRTs suggests that object identity only matters during the discrimination phase of target-distractor competition. Thus, once the distractor is fully inhibited and the competition process is complete, the effect of similarity on saccade angle is simply linear.

Overall, a more complex object-based suppressive surround may exist like it does for simple features, but only during the discrimination phase of target-distractor competition. Complex features have been found to be processed by the inferotemporal (IT) cortex, an area that can discriminate between complex targets and distractors (Baylis & Rolls 1987; Miller et al. 1993; Tanaka, 2003), compared to the SC and FEF which are only capable of discriminating simple features (Kehoe et al., 2018a). The difference in brain regions and stages of visual processing involved in target-distractor competition for simple versus higher order features could further explain our finding. Although we found evidence of a suppressive surround in object space for endpoint deviation, we did not see the same effects on initial angle or the curvature metrics. To further understand the differences in metrics and establish concrete evidence of a complex object-based suppressive surround, further analysis on the effects of target-distractor similarity at varying SRTs would need to be done.

Kehoe et al. (2018a) tested the effects of similarity, using the same stimuli, on saccade curvature with a target and two distractor objects placed 45° from each other. They found that as the similarity between the target and most similar distractor object decreased (as OS increased), the saccade curvature (sum and max curvature) and endpoint deviation angle increased linearly. To compare the present study with that of Kehoe et al. (2018a), we examined the saccade metrics across similarity for the subset of trials with the distractor at 45° (AD = 2), analyzing them using linear regressions. For short SRTs, we did not see any significant linear patterns. For long SRTs, we found that mean endpoint deviation angle significantly increased as similarity decreased (R^2 = 0.97, p = 0.02). Initial angle and sum curvature also followed the same linear relationship although not statistically significant (R^2 = 0.76, p = 0.13; R^2 = 0.80, p = 0.11, respectively). The lack of statistical significance for the linear regressions over initial angle and sum curvature was most likely due to a lack of statistical power. Since we varied AD throughout the experiment, conditions with AD = 2 occurred about $1/5^{th}$ as many times as in Kehoe et al. (2018a). It is likely these results would be significant with more data from trials with AD = 2. Therefore, our findings at 45° are qualitatively consistent with Kehoe et al. (2018a) and would likely replicate their results with more statistical power.

4.6.4 Interaction of angular distance and similarity

While we had hypothesized that the effects of similarity on saccade trajectories would be affected in a multiplicative fashion through AD, we found no such significant interactions. This suggests that spatial layout and object similarity are independently processed and incorporated into oculomotor planning. We found that when target-distractor competition was actively underway, AD effects showed evidence of weighted saccade averaging and incomplete winner-take-all, whereas the similarity effects were consistent with a suppressive surround pattern of

inhibition seen for endpoint deviation. The similarity between competing objects matters most during this discrimination phase, where object-based suppressive surrounds are activated to aid in distractor inhibition. Once the target-distractor competition process has been fully resolved and the objects have been discriminated, a spatial suppressive surround is activated resulting in the effects of AD on saccade trajectory. Thus, the stage of development of the target-distractor competition process gives rise to independent suppressive effects either through similarity or AD.

As well, the effects of AD on saccade trajectory were more robust than the effects of similarity. AD affected the whole saccade (all metrics) whereas similarity mainly affected initial and endpoint deviation angle. Additionally, the effects of AD were greater in magnitude compared to similarity, as evidenced by greater and significant differences between conditions shown in Figure 4.5 compared to Figure 4.6, as well as in statistical analysis (see Table 4.2). The effects of AD on the metrics were similar in magnitude between short and long SRTs, except for endpoint deviation and angle at max curvature where AD had a larger effect at short SRTs than long SRTs. Overall, SRT had the greatest effect on the metrics, and then AD, whereas similarity had the least effect.

4.6.5 Relationship to current oculomotor circuitry and target selection literature

This study demonstrates that varying the distance versus the similarity of complex objects, and the timing of the competition process affect target selection and saccade planning in different ways. Saccades initiated during the early stages of target-distractor competition (short SRTs) exhibit weighted saccade vector averaging caused by the enhanced neural activity of the oculomotor neuron populations encoding the two saccade goals (Port & Wurtz, 2003; Godjin & Theeuwes, 2002; Findlay & Walker, 1999). The final saccade motor plan is a result of

reweighting the possible saccade goals based on their behavioural relevance and priority, which for this task is the similarity of the objects in question to the remembered target object displayed at the start of the trial (Kehoe et al., 2018a). On-line corrections (displayed through saccade curvature) pull the saccade towards the target when it is initially planned to land at a weighted average of the object locations. With more time (long SRTs), the target-distractor competition resolves causing the population of neurons encoding the unchosen saccade goal to decrease in activity (McPeek et al., 2003; McPeek, 2006; White et al., 2012). Suppressive surrounds develop around the attended target and inhibit the distractor causing the subsequent saccade vector to point away from the distractor.

We found evidence of both the early and late stages of the target selection process when varying AD. The spatial layout of the objects in the visual field is encoded in the oculomotor system through attentional priority maps where neurons encoding objects of interest (through both bottom-up and top-down features) have increased activity (Fecteau & Munoz, 2006; White et al., 2017; Fernandes et al., 2013). With sufficient time, the suppressive zone surrounding the attentional spotlight centred at a target object develops in the oculomotor system. Many studies have shown a link between spatial attention and oculomotor areas (Moore & Fallah, 2001; Moore & Fallah 2003; Moore et al., 2003), which suggests that spatial surround suppression developed in visual processing areas feeds into attentional priority maps in the oculomotor system (such as through feedback between the dorsal stream and FEF) to create oculomotor plans that aim saccades to the desired object. We also showed that distractor inhibition occurred when varying the similarity of our complex, novel stimuli. Complex visual information is processed in later regions of the ventral stream, such as the IT cortex in areas TE and TEO (Baylis & Rolls 1987; Miller et al. 1993; Tanaka, 2003). Although our target and distractor

objects are processed and discriminated in these regions of higher order processing of the ventral stream, the visual information regarding similarity would project to the oculomotor system for saccade planning and distractor inhibition. Therefore, spatial layout and object similarity are processed in their respective visual processing areas, and then distance and similarity information are fed into the oculomotor system, combining with attentional priority maps to create oculomotor plans.

4.6.6 Conclusion

In conclusion, we examined the effects of varying both AD and similarity in a visual search task using novel, complex objects, whereas previous studies have kept the distractor at a fixed distance to the target in this type of target selection task. We showed that there was a clear distinction between saccade angle and saccade curvature through the timing of the switch from being positively to negatively deviated (the curvature metrics flipped signs slightly earlier than the angle metrics), as well as the ways in which they were affected by AD. Our results reflect what has been shown for smooth pursuit eye movements where the initial processes emulated weighted vector averaging whereas the later processes reflected a winner-take-all (Recanzone & Wurtz, 1999). We found that AD had a strong influence on saccade trajectories and that the effect of similarity is limited. After sufficient time to allow for distractor inhibition, the effects of AD on saccade angle and curvature were consistent with a spatial suppressive surround gradient around the attended target item, whereas without enough time, the effects followed spatial averaging and incomplete winner-take-all. In comparison, similarity modulated endpoint deviation in a similar suppressive surround shape. As well, similarity affected initial angle for longer SRTs showing evidence of a linearly modulated suppressive zone. Many studies have observed feature-based suppressive surrounds for simple features such as colour, orientation, and

direction of motion, and we have provided some evidence of a complex object-based suppressive surround during the discrimination phase of target-distractor competition. Lastly, we did not find any interaction effects between spatial and complex featural discrimination despite simultaneously varying them in our task, suggesting that these variables are processed by independent neural circuitry. We suggested that after distance and similarity are processed in their respective higher order visual processing areas, both sets of visual information likely combine with attentional priority maps in the oculomotor system for final saccade plans to be created.

Chapter 5: Pupillometry

5.1 Introduction

Pupil size changes with varying factors: arousal, light, cognitive load, and attention. Pupillary changes with respect to arousal are tied to the sympathetic nervous system, where the fight-or-flight response causes the pupil to dilate to increase the visual signal to better see the surrounding environment (Aston-Jones et al., 1984; McDougal & Gamlin, 2008; Kardon, 2005). On the other hand, when bright light enters the retina, the pupil contracts due to the pupillary light reflex (Hakerem, 1967). The effects of cognitive load and attention are more recent findings, but they can often connect to the pupillary response to light. Studies have shown that covertly attending to brighter objects can induce the pupillary light reflex and cause pupil constriction (Binda et al., 2013; Mathôt et al., 2013; Tkacz-Domb & Yeshurun, 2018), even though there is no actual change in light entering the pupil. An attentional-cueing study by Mathôt et al. (2013) showed that covertly attending to a cued white location on a display caused pupil size to decrease compared to covertly attending to a cued dark location on the display. This study demonstrated the connection between attention and the pupillary response. Pupil size has also been shown to be affected by cognitive workload, where increasing the difficulty of the task causes the pupil to dilate to increase the visual signal (Laeng et al., 2012; Hess & Polt, 1964).

Since spatial attention is deployed by the oculomotor system (Moore & Fallah, 2001; Moore & Fallah, 2004; Moore at al., 2003), we hypothesized that there may also be a link between target-distractor competition and the pupillometry system. We expected that the competitive interactions we found for targets and distractors on saccade trajectories would be reflected in the control of pupil size. We performed an analysis of pupil size data taken from a

target selection task to assess the role of competition on pupillary responses and the similarities between these effects with those found for saccades.

Our saccade trajectory analysis from Chapter 4 showed a series of results at short and long saccadic reaction times (SRTs) that differed when varying angular distance (AD) and objective similarity (OS). We expected that during the periods of fixation before and after display onset, we would find effects of AD and OS on pupil size that reflected our saccade results. We examined four periods of fixation: before display onset, after display onset, before saccade initiation, and post-saccade fixation. We expected that before display onset, there would be no effect of our variables on pupil size since the target and distractor were not yet presented, and therefore there was no competition. In the period after display onset, we expected that there would be an effect of AD on pupil size but not similarity since the object identities had not been fully processed. At the closest AD, the distractor was in the attentional focus zone of the target, which would cause pupil constriction based on prior attentional pupillometry studies (Tkacz-Domb & Yeshurun, 2018). This effect would drop off as AD increased. We hypothesized that during the period before saccade initiation, we would find effects of AD and similarity on pupil size consistent with our spatial suppressive surround and linear effects shown for saccades made with long SRTs in Chapter 4. During the period of post-saccade fixation, we expected to see the effects of fully resolved competition between the target and distractor. Taken together, finding effects of target-distractor competition on pupil size consistent with our findings for saccade trajectories would suggest that top-down connections to the subcortical pupillometry system receive input from the parts of the oculomotor system that encode saccade trajectories.

5.2 Methods

This study examined pupillometry during the fixational periods before and after saccades using data from the study described in Chapter 4.

5.2.1 Analysis

5.2.1.1 Pupil area over time: Pupil area was recorded every 2ms from central fixation cross onset after target preview until the end of the trial after object fixation (Figure 5.2). Pupil area has arbitrary units as stated in the EyeLink II user manual. Trials were grouped by angular distance (AD) or objective similarity (OS) conditions. The pupil size data across each trial was averaged within each AD or OS condition and plotted across time from baseline fixation onset to 1000ms after fixation onset. 1000ms was used to ensure we captured the changes in pupil size at least 200ms after post-saccade target fixation.

5.2.1.2 Time periods: The data was split into 4 time periods: 1) baseline 200ms during initial fixation; 2) first 100ms after target/distractor onset; 3) last 100ms before saccade onset; and 4) 200ms post-saccade during target fixation. These 4 periods were analyzed separately by short and long SRTs due to the differences seen with saccade trajectories in Chapter 4.

5.2.1.3 Average pupillometry: We examined how pupil size changed as AD and OS were varied within the 4 time periods. The data was normalized per participant by the maximum time-averaged pupil size amongst the 5 AD x 4 OS x 2 SRT periods conditions. Linear regressions were performed on the averaged normalized data across AD and OS. Goodness of fit metrics (R^2 and p-value) are provided. For each time period, a 5 AD x 4 OS univariate ANOVA was performed in SPSS, for short and long SRTs separately. Scheffe post-hoc analysis was used to investigate significant effects across conditions.

5.3 Results

Plotting the average pupil area across time from the start of the baseline period to 1000ms after showed an initial increase in pupil size. This could be related to the cognitive load required to resolve target-distractor competition, causing the pupil to dilate to increase the visual signal. At about 600ms, the pupil size was at its peak and then it decreased. Looking at the lines for angular distance (AD) and objective similarity (OS), OS 1 and 2 were separated from OS 3 and 4. Despite this, there were no significant differences between AD (Figure 5.1 A) or OS (Figure 5.1 B) conditions, as evidenced by overlapping shaded SEM regions. Therefore, the lack of significant differences suggests that varying distance and similarity had no effect on pupil size in this task.

Plotting the normalized average pupil size across AD and OS for each of the four time periods split by short and long SRTs showed no significant differences in pupil size between conditions (Figure 5.2 A, B). The linear regressions performed did not show statistical significance since the trendlines were relatively horizontal with overlapping SEM error bars. For all four periods and all conditions (AD/short SRTs, AD/long SRTs, OS/short SRTs, OS/long SRTs), the ANOVAs performed showed no significant main effects or interactions. Therefore, there were no effects of varying AD or OS on pupil size during any of the relevant time periods analyzed.

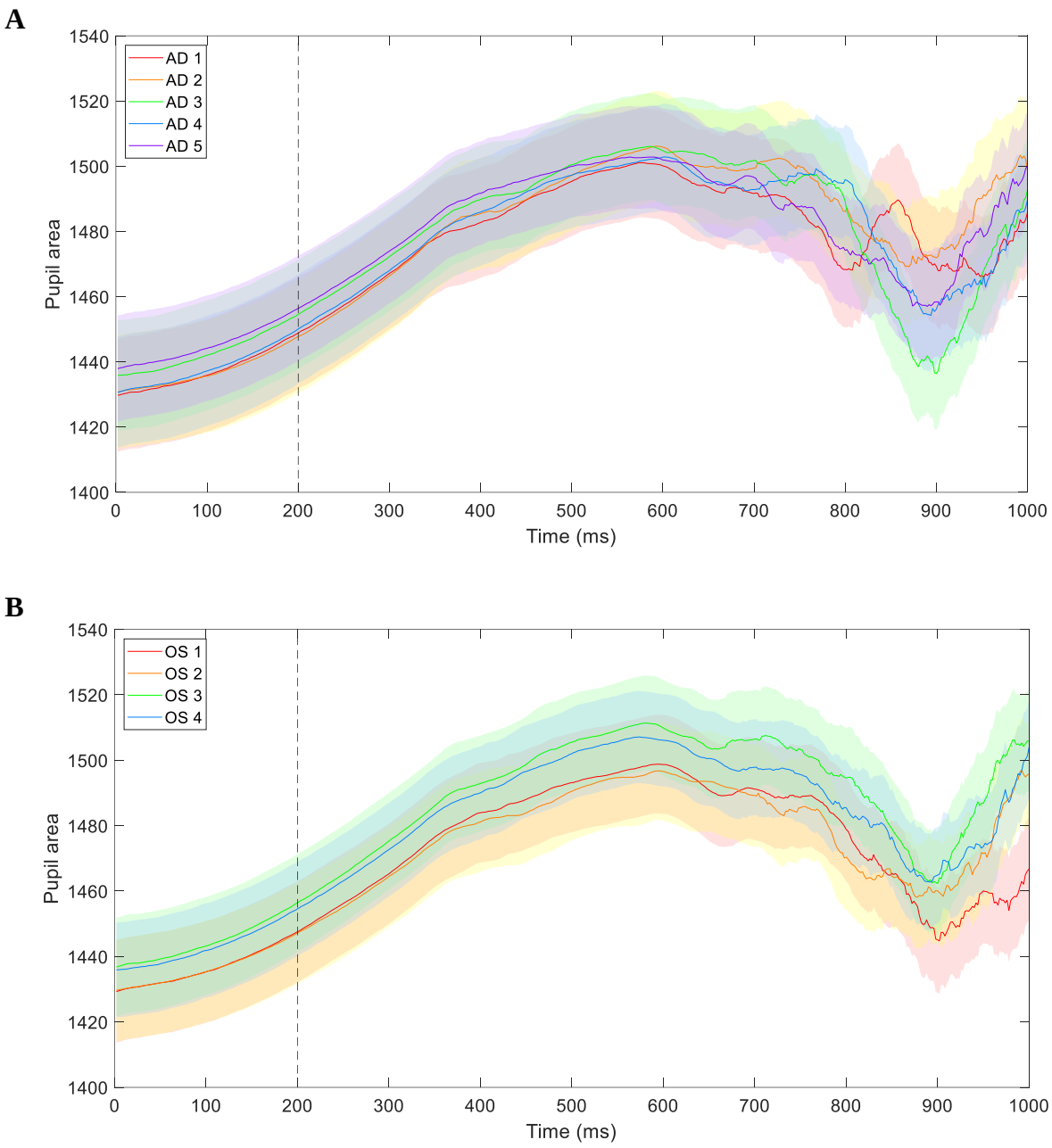

Figure 5.1. Average pupil area over time split by angular distance (AD) and objective similarity (OS). Pupil area units are arbitrary as stated by the EyeLink II user manual. Shaded regions are SEM. The black dashed line represents display onset. *A*: Pupil area split by AD. *B*: Pupil area split by OS.

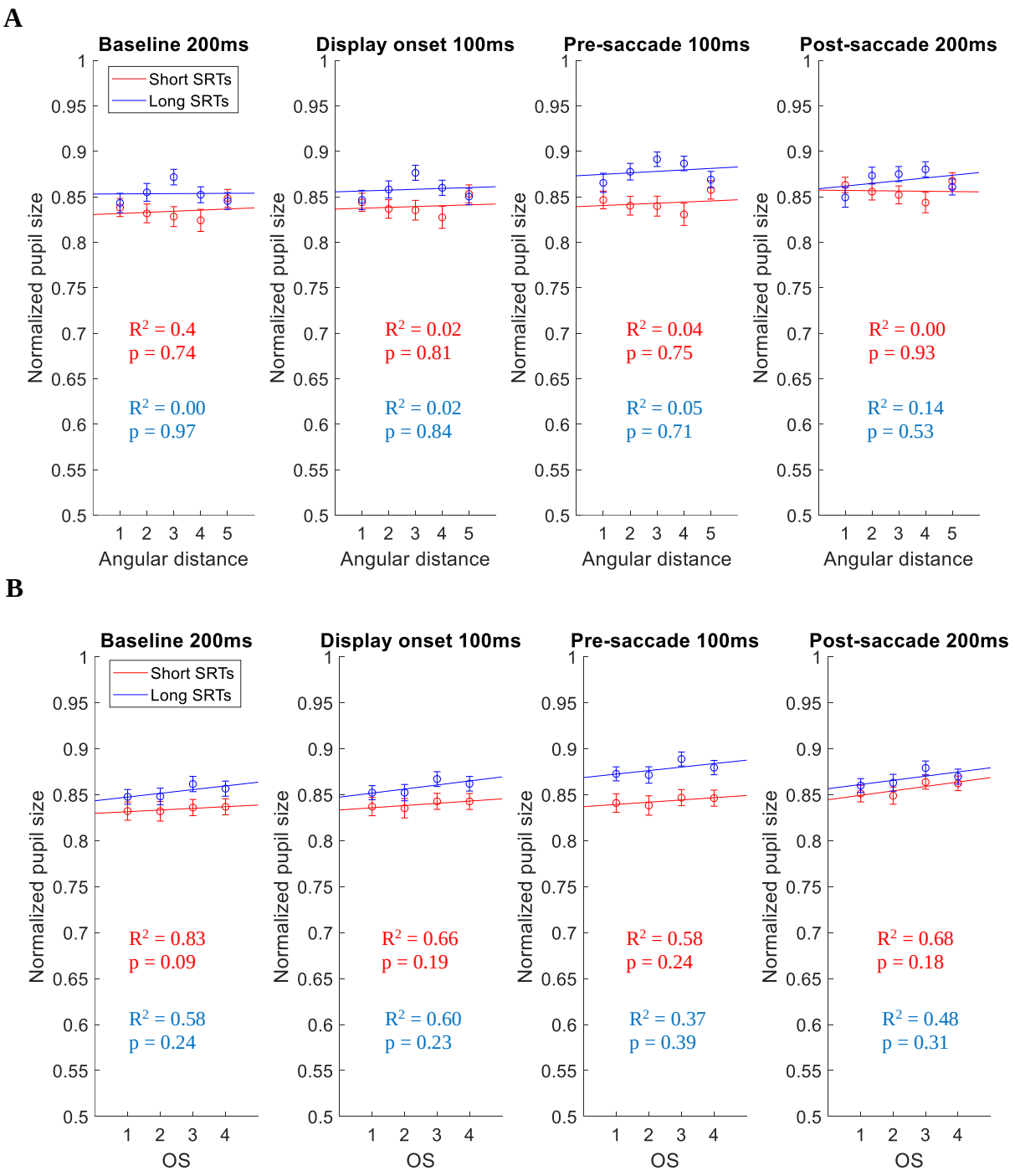

Figure 5.2. Average normalized pupil size over angular distance (AD) and objective similarity (OS). Trial data was split into short and long saccadic reaction times (SRTs) shown in red and blue, respectively. Linear regressions are shown with trendlines and respective R^2 and p-values by colour. Values were plotted for each of the four time periods. Error bars are SEM. *A*: Pupil size over AD. *B*: Pupil size over OS.

5.4 Discussion

We examined the effect of varying angular distance and similarity on pupil area from a target selection task. We hypothesized that if the oculomotor circuitry that produced changes in saccade trajectory due to spatial and object-based competition was also part of the top-down control of pupil size, we would see the results of target-distractor competition seen for saccade trajectories reflected in the pupillary response. However, we did not find any significant differences between conditions of angular distance, similarity, or time period of fixation on pupil size. Thus, there is no evidence that competing saccade plans influence pupillometry as they do for saccade trajectories.

These null results suggest that the broader oculomotor system, especially with respect to saccade competition and attentional priority maps, does not feed into the subcortical pupillometry system. More likely, the top-down connections to the pupillometry system are solely focused on the winning, and covertly attended saccade vector, guided by input regarding the luminance of the target object. A hypothetical explanation for this could be that the thalamic nuclei responsible for driving arousal receive input from areas of visual processing in the early and middle ventral stream, as highlighted by covert spatial attention. These thalamic nuclei connect to the brainstem and would allow the slow pupil response to proactively start changing in advance of shifting gaze to the target. It would also be possible that the mechanism driving the pupillary response completely bypasses the frontal eye field and superior colliculus, missing any information regarding target-distractor competition and attentional priority. Therefore, pupil size changes would not be tied back to the same competition processes that influence saccade trajectories. Future studies would be needed to determine the neural circuitry for top-down pupillary control, as well as where and how it interacts with saccade planning.

Chapter 6: General Discussion

6.1 General Discussion

We examined the effects of target-distractor competition on saccade trajectories and pupil size and addressed the questions and hypotheses posed in Chapter 3. Using a target selection task, we varied the angular distance (AD) and objective similarity (OS) between complex target and distractor objects. In Chapter 4, we used a variety of metrics to measure the effect of these variables on saccade trajectories. We found that the effect of AD and similarity on saccade shape varied with increasing saccadic reaction time (SRT): for short SRTs, saccades were pointed towards the distractor and for long SRTs, saccades were pointed away from the distractor, suggesting distractor suppression. This finding is consistent with previous research and is indicative of the development of the target-distractor competition process (McSorley et al., 2006; Walker et al., 2006). For trials with short SRTs, we found that varying AD modulated saccade trajectories consistent with weighted saccade vector averaging and an incomplete winner-take-all process. When varying similarity, we found evidence of an object-based suppressive surround in endpoint deviation, where distractors at middle similarity levels were suppressed more than those more and less similar. These results at short SRTs are consistent with an incomplete competition process where the distractor had not yet been fully suppressed. At long SRTs, there was enough time to fully resolve the target-distractor competition and inhibit the distractor. For these trials, we observed the pattern of a spatial suppressive surround for all saccade metrics when varying AD. We also found that when the objects were less similar, it was easier to inhibit the distractor object, as shown through the linear trend of initial angle. Lastly, we did not find any evidence of interactions between the found effects of AD and similarity on saccade trajectories.

Looking at our pupillometry analysis from Chapter 5, we did not find any evidence of target-distractor distance or similarity modulating pupil size during the periods of fixation from our target selection task. We did find that pupil size increased after display onset. Typically, an increase in brightness due to display onset would cause the pupil to constrict, but since we found pupil dilation, it suggests the task increased cognitive load and required more attention. Aside from this, there were no significant differences of pupil size between angular distances or similarity levels. As well, there were no significant interactions between these variables. These null results suggest that top-down connections from the oculomotor system regarding target-distractor competition do not feed into the subcortical pupillometry system.

In Chapters 4 and 5, we did not find evidence of any interactions between the effects of AD and similarity on saccades or pupil size through statistical analyses. Despite these results, we did find qualitative support that AD and similarity interact with each other. We produced heat maps over AD and similarity where the heat/colour represents the value of the saccade metric from negative to positive deviations (Figure 6.1). We found that there was a hot spot of interaction at OS= 3, AD = 3 for the three curvature metrics, that was mirror symmetric across short and long SRTs. At short SRTs, the coordinate (3, 3) displayed the most curvature towards the distractor, whereas at long SRTs, the coordinate (3, 3) displayed the most curvature away from the distractor. As well, at OS = 3, AD = 4, there was the opposite pattern for the curvature metrics with low deviation towards versus away from the distractor at short and long SRTs respectively. The consistent patterns at these coordinates suggest there may be an interaction between AD and similarity that there was not enough statistical power to see, due to the number of conditions and limit to a single 1-hour experimental session. A multi-session experiment to

increase the number of trials at all combinations would be needed to follow up on this intriguing qualitative result.

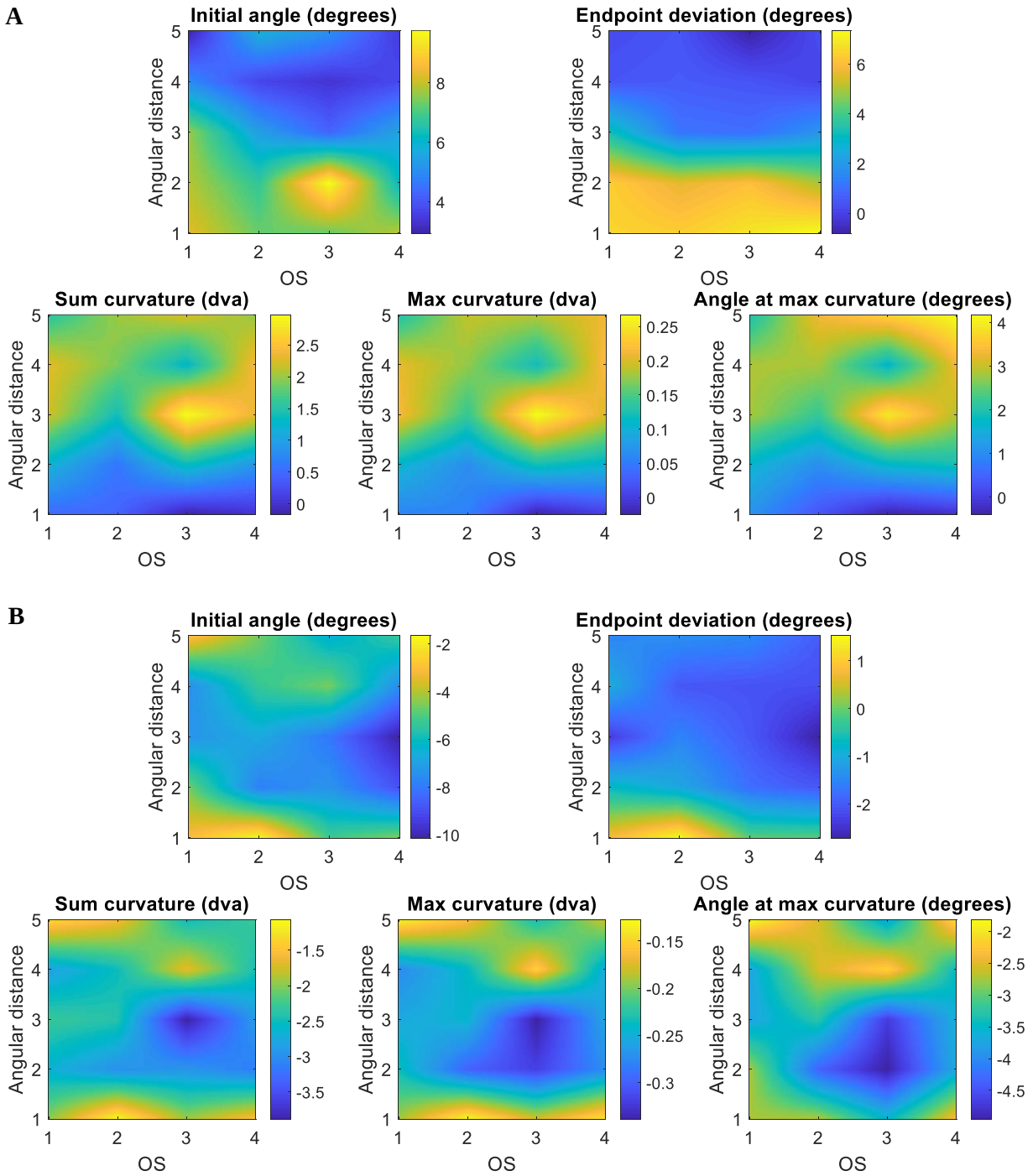

Figure 6.1. Heat maps over angular distance and similarity for each saccade metric at short and long saccadic reaction times (SRTs). The heat/colour is the metric value. *A:* Heat maps at short SRTs. *B:* Heat maps at long SRTs.

As outlined in Chapter 4, we saw distinct effects of short versus long SRTs, as well as target-distractor AD versus similarity on saccade trajectories. Our results and the patterns we found give us more information about the neural pathways involved to produce these effects and elucidate the inner-workings of the target-distractor competition process. At short SRTs, we found early effects of AD and similarity on saccade trajectories. Saccades made with short SRTs were initiated before the target-distractor competition resolved and while the objects were still being discriminated from one another. For AD, we found that saccades made during this early phase of the competition process reflected weighted saccade vector averaging and an incomplete winner-take-all (Port & Wurtz, 2003; Godjin & Theeuwes, 2002; Findlay & Walker, 1999). As depicted by the red arrows in Figure 6.2, we proposed that these early effects are driven mainly by the oculomotor system. More specifically, the frontal eye field (FEF) would receive visual information regarding object space and location from the dorsal stream, such as from the posterior parietal cortex (PPC). We found evidence of an object-based suppressive surround in the effects of similarity for endpoint deviation angle during the early, discrimination phase of the competition process. This finding is consistent with feature-based suppressive surrounds that have been found for simple features, such as colour, direction of motion, and orientation (Tsotsos et al., 2005; Tombu & Tsotsos, 2008; Störmer & Alvarez, 2014; Yoo et al. 2018). To explain our results, we suggested that visual information regarding complex object features is projected from the ventral stream, or more specifically TE and TEO, to the oculomotor system (as seen with the blue arrows in Figure 6.2). The brainstem then drives the output of a saccade. Although there have been studies suggesting connections between the ventral stream and the superior colliculus (SC) (Wang & Burkhalter, 2013; White et al., 2009), it has not been shown that areas TE and TEO directly connect to SC as we have depicted in our figure. As well, we depicted the early

phase of competition with dashed arrows to signify the unresolved competition between saccade goals.

During the late phase, seen for trials with long SRTs, target-distractor competition had been fully resolved. The distractor could be fully inhibited, and saccades pointing away from the distractor were seen. We found that AD modulated saccade trajectory shape in a pattern consistent with a DoG-shaped spatial suppressive surround (Tsotsos, 1990; Tsotsos et al., 1995; Cutzu & Tsotsos, 2003; Hopf et al., 2006); there was the most distractor suppression when it was placed at a medium distance from the target. The spatial suppressive surround is driven by reciprocal connections between the dorsal stream (PPC) and the FEF (Figure 6.2). These effects are further established by the oculomotor system, or more specifically the FEF and SC, where the activity of neural populations encoding both saccade goals is increased or decreased based on the suppressive zone (McPeek & Keller, 2001; McPeek et al., 2003; Port and Wurtz, 2003). During this late phase of the competition process, the activity encoding the distractor is suppressed below a baseline level, causing the outputted saccade to deviate away from the distractor (Doyle & Walker, 2001, 2002; McSorley et al., 2004; White et al., 2012). As for the effects of similarity on saccade trajectories during the late phase, we found that initial angle was modulated linearly suggesting that as the target and distractor become less similar, it is easier to inhibit the distractor. We suggested the neural pathway shown for the early phase is the same for the late, but with a sign change from positive to negative, where there is more distractor suppression resulting in saccade deviation away from the object in the late phase. The arrows in the late depiction of Figure 6.2 are solid to signify the completion of the competition process.

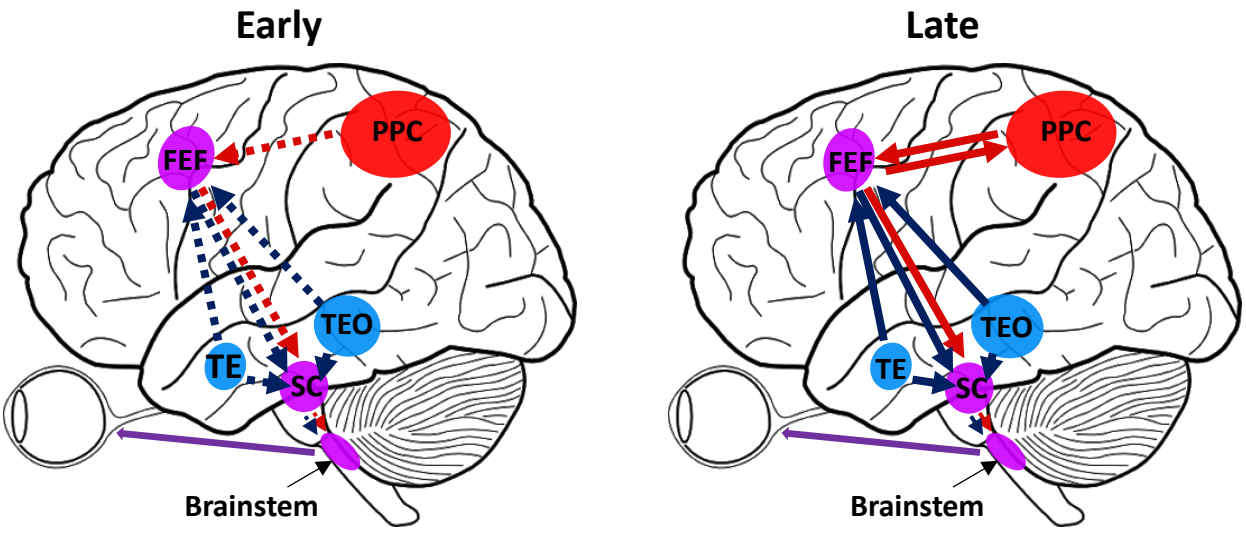

Figure 6.2. Early versus late neural pathways involved in target-distractor competition. Dashed arrows represent unresolved competition whereas solid arrows represent complete competition. Red and blue arrows depict the potential pathways involved when angular distance versus similarity affects saccades, respectively. This diagram depicts the connections of the ventral (blue areas) and dorsal (red area) streams to the oculomotor system (purple areas). The connections from TE/TEO to SC may not be direct, but connections between the ventral stream and SC have been determined.

To test the pathways we proposed above, we would need to conduct neural recording studies where we simultaneously record from the specified regions while participants performed a target selection task. These neural recordings would give us direct evidence of the pathways involved in the early and late phases of target-distractor competition, as well as how angular distance and complex object similarity integrate into the oculomotor system. Through these studies, we could see the competition and motor plans evolve dynamically over time producing the results we found. To fully understand how target-distractor distance modulates saccade trajectories, another future study would be to examine how distance varying in an allocentric reference frame affects saccade trajectories. This would be done by varying the target-distractor distance by length, rather than by angular distance in an egocentric reference frame, as we did in

Chapter 4. Previous research has shown that the dorsal stream requires visual information to be coded in an egocentric reference frame for motor planning and control, whereas the ventral stream uses an allocentric reference frame (Milner & Goodale, 1995; Dijkerman et al., 1998). Therefore, this future work would teach us more about how the brain encodes both reference frames with respect to saccade vectors and motor plans during target-distractor competition.

Considering potential caveats of our studies from Chapters 4 and 5, it is important to note that the bulk of our analyses examined correct trials where participants made a saccade to the target object. Since our task involved only two competing objects, some of these correct trials were due to chance, which would minimize the effects we were expecting to observe. Therefore, if we were able to decrease the percentage of correct trials due to chance, this could influence our findings. For instance, our results for similarity could be enhanced with a task design that leaves less of an opportunity to guess which object is the target. This way, most of the correct trials would occur after discriminating the objects and determining which is the target before initiating a saccade.

6.2 Conclusion

The studies provided in this thesis examined the effects of distance and complex object similarity on the target-distractor competition process. This process is reflected in saccade trajectories made to the target, but not in pupil size during the periods of fixation from our task. The results of these studies have implications to the broader field of eye movement research, especially regarding the oculomotor system. They provide us with more information about how distance and similarity information may be processed, and possibly integrated to create saccade plans, as well as the timing of these processes. This thesis demonstrates that the dorsal and ventral streams feed forward different information to the oculomotor system depending on the

stage of the target-distractor competition process at the time of saccade initiation. These pathways also depend on what type of visual information is being processed: spatial or complex object information. Altogether, this thesis contributes to our knowledge of the effects of target-distractor competition on the oculomotor system.

References

Albano JE, Norton TT, Hall WC. Laminar origin of projections from the superficial layers of the superior colliculus in the tree shrew, *Tupaia glis*. *Brain Res* 173: 1-11, 1979.

Anderson RA, Asanuma C, Cowan WM. Colossal and prefrontal associational projecting cell populations in area 7A of the macaque monkey: A study using retrogradely transported fluorescent dyes. *J Comp Neurol* 232: 443-455, 1985. doi: 10.1002/cne.902320403.

Apter JT. Projection of the retina on superior colliculus of cats. *J Neurophysiol* 8: 123-134, 1945.

Aston-Jones G, Foote SL, Bloom FE. Anatomy and physiology of locus coeruleus neurons: Functional implications. In: *Norepinephrine: Frontiers of Clinical Neuroscience*, edited by Ziegler M and Lake CR. Baltimore: Williams & Wilkins, vol. 2, p. 92-116, 1984.

Bahill AT, Stark L. Oblique saccadic eye movements. *Arch Ophthalmol* 95: 1258-1261, 1977.

Baylis GC, Rolls ET. Responses of neurons in the inferior temporal cortex in short term and serial recognition memory tasks. *Brain Res* 65: 614-622, 1987.

Bex PJ, Bedingham S, Hammett ST. Apparent speed and speed sensitivity during adaptation to motion. *J Opt Soc Am A* 16: 2817-2824, 1999.

Binda P, Pereverzeva M, Murray SO. Attention to bright surfaces enhances the pupillary light reflex. *J Neurosci* 33. 2199-2204, 2013.

Bizzi E. Discharge of frontal eye field neurons during saccadic and following eye movements in unanesthetized monkeys. *Exp Brain Res* 6: 69-80, 1968. doi: 10.1007/BF00235447.

Bruce CJ, Goldberg ME. Primate frontal eye fields. I. Single neurons discharging before saccades. *J Neurophysiol* 53: 603-635, 1985.

Bruce CJ, Goldberg ME, Bushnell MC, Stanton GB. Primate frontal eye fields. II. Physiological and anatomical correlates of electrically evoked eye movements. *J Neurophysiol* 54: 714-734, 1985.

Buttner-Ennever JA, Buttner U. A cell group associated with vertical eye movements in the rostral mesencephalic reticular formation of the monkey. *Brain Res* 151: 31-47, 1978.

Buttner U, Buttner-Ennever JA, Henn V. Vertical eye movement related unit activity in the rostral mesencephalic reticular formation of the alert monkey. *Brain Res* 130: 239-252, 1977.

Butts DA, Goldman MS. Tuning curves, neuronal variability, and sensory coding. *PLos Biol* 4: e92, 2006.

Castelo-Branco M, Formisano E, Backes W, Zanella F, Neuenschwander S, Singer W, Goebel R. Activity patterns in human motion-sensitive areas depend on the interpretation of global motion. *Proc Natl Acad Sci* 99: 13914–13919, 2002.

Cavada C, Goldman-Rakic PS. Posterior parietal cortex in rhesus monkey: II. Evidence for segregated corticocortical networks linking sensory and limbic areas with the frontal lobe. *J Comp Neurol* 287: 422-445, 1989. doi: 10.1002/cne.902870403.

Cohen B, Henn V. Unit activity in the pontine reticular formation associated with eye movements. *Brain Res* 46: 403–410, 1972.

Cohen B, Komatsuzaki A. Eye movements induced by stimulation of the pontine reticular formation: Evidence for integration in oculomotor pathways. *Exp Neurol* 36: 101-117, 1972.

Colby C, Goldberg M. Space and attention in parietal cortex. *Annu. Rev. Neurosci.* 22: 319-349, 1999. doi: 10.1146/annurev.neuro.22.1.319.

Costello MG, Zhu D, Salinas E, Stanford T. Perceptual modulation of motor – but not visual – responses in the frontal eye field during an urgent-decision task. *J Neurosci* 33: 16394-16408, 2013. doi: 10.1523/JNEUROSCI.1899-13.2013.

Curthoys IS, Markham CH, Furuya N. Direct projection of pause neurons to nystagmus-related excitatory burst neurons in the cat pontine reticular formation. *Exp Neurol* 83: 414-422, 1984.

Cutzu F, Tsotsos JK. The selective tuning model of attention: psychophysical evidence for a suppressive annulus around an attended item. *Vision Res* 43: 205-219, 2003.

Desimone R, Duncan J. Neural mechanisms of selective visual attention. *Annu Rev Neurosci* 18: 193-222, 1995. doi: 10.1146/annurev.ne.18.030195.001205.

DeYoe EA, Van Essen DC. Concurrent processing streams in monkey visual cortex. *Trends Neurosci* 11: 219-226, 1988.

Dijkerman HC, Milner AD, Carey DP. Grasping spatial relationships: Failure to demonstrate allocentric visual coding in a patient with visual form agnosia. *Conscious Cogn* 7: 424-437, 1998.

Dow BM. Functional classes of cells and their laminar distribution in monkey visual cortex. *J Neurophysiol* 37: 927-940, 1974.

Downing P, Jiang Y, Shuman M, Kanwisher NA. Cortical area selective for visual processing of the human body. *Science* 293: 2470-2473, 2001.

Duffy CJ. MST Neurons respond to optic flow and translational movement. *J Neurophysiol* 80: 1816-1827, 1998.

Ebitz RB, Moore T. Both a gauge and a filter: Cognitive modulations of pupil size. *Front. Neurol.* 9: 1190, 2019. doi: 10.3389/fneur.2018.01190.

Ebitz RB, Moore T. Selective modulation of the pupil light reflex by microstimulation of prefrontal cortex. *J Neurosci* 37: 5008-5018, 2017. doi: 10.1523/JNEUROSCI.2433-16.2017.

Edwards SB, Ginsburgh CL, Henkel CK, Stein BE. Sources of subcortical projections to the superior colliculus in the cat. *J Comp Neur* 184: 309-330, 1979.

Evinger C, Kaneko CR, Fuchs AF. Activity of omnipause neurons in alert cats during saccadic eye movements and visual stimuli. *J Neurophysiol* 47: 827–844, 1982.

Fallah M, Reynolds JH. Contrast dependence of smooth pursuit eye movements following a saccade to superimposed targets. *PLoS ONE* 2012: e37888, 2012. doi: 10.1371/journal.pone.0037888.

Fecteau JH, Munoz DP. Salience, relevance, and firing: A priority map for target selection. *Trends Cogn Sci* 10: 382-390, 2006. doi: 10.1016/j.tics.2006.06.011.

Feldman JA. Dynamic connections in neural networks. *Biol Cybern* 46: 27-39, 1982.

Felleman DJ, Xiao Y, McClendon E. Modular organization of occipito-temporal pathways: cortical connections between visual area 4 and visual area 2 and posterior inferotemporal ventral area in macaque monkeys. *J Neurosci* 17: 3185-3200, 1997.

Fernandes HL, Stevenson IH, Phillips AN, Segraves MA, Kording KP. Saliency and saccade encoding in the frontal eye field during natural scene search. *Cereb Cortex* 24: 3232-3245, 2013. doi: 10.1093/cercor/bht179.

Findlay JM, Harris LR. Small saccades to double-stepped targets moving in two dimensions. In: *Theoretical and Applied Aspects of Eye Movement Research*, edited by Gale AG and Johnson F. Amsterdam: Elsevier, p. 71-78, 1984.

Findlay JM, Walker R. A model of saccade generation based on parallel processing and competitive inhibition. *Behav Brain Sci* 22: 661-721, 1999. doi: 10.1017/S0140525X99002150.

Gamlin PD. The pretectum: Connections and oculomotor-related roles. *Prog Brain Res* 151: 379-405, 2006.

Godjin R, Theeuwes J. Progamming of endogenous and exogenous saccades: Evidence for a competitive integration model. *J Exp Psychol* 28: 1039-1054, 2002. doi: 10.1037//0096-1523.28.5.1039.

Godijn R, Theeuwes J. The relationship between inhibition of reture and saccade trajectory deviations. *J. Exp. Psychol.* 30: 538-554, 2004. doi: 10.1037/0096-1523.30.3.538.

Goldberg ME, Wurtz RH. Activity of superior colliculus in behaving monkey. I. Visual receptive fields of single neurons. *J Neurophysiol* 35: 542-559, 1972.

Goodale MA, Milner AD. Separate visual pathways for perception and action. *TINS* 15: 20-25, 1992.

Hakerem G. Pupillography. In: *A manual of psychophysiological methods*, edited by Venables PH and Martin I. Amsterdam: North-Holland Publishing Co., p. 335-349, 1967.

Hall WC, Moschovakis A. The superior colliculus: New approaches for studying. In: *Methods and new frontiers in neuroscience*, edited by Hall WC, Moschovakis A. Boca Raton: CRC Press LLC, 2004.

Hammett ST, Thompson PG, Bedingham S. The dynamics of velocity adaptation in human vision. *Curr Biol* 10: 1123-1126, 2000.

Hanes DP, Schall JD. Neural control of voluntary movement initiation. *Science* 274: 427-430, 1996.

Harting JK, Huerta MF, Hashikawa T, van Lieshout DP. Projection of the mammalian superior colliculus upon the dorsal lateral geniculate nucleus: organization of tectogeniculate pathways in nineteen species. *J Comp Neurol* 304: 275-306, 1991.

Heitz RP, Schall JD. Neural mechanisms of speed-accuracy tradeoff. *Neuron* 76: 616-628, 2012.

Henik A, Rafal R, Rhodes D. Endogenously generated and visually guided saccades after lesions of the human frontal eye fields. *J Cog Neursci* 6: 400-411, 1994.

Hess WR, Burgi S, Bucher V. Motorisch Funktion des Tektal und Temgentalgebietes. *Monatsschr Psychiatr Neurol* 112: 1-52, 1946.

Hess EH, Polt JM. Pupil size in relation to mental activity during simple problem-solving. *Science* 143:1190–1192, 1964.

Hickey C, van Zoest W. Reward creates oculomotor salience. *Curr Biol* 22: 219-220, 2012.

Hopf JM, Boehler CN, Luck SJ, Tsotsos JK, Heinze HJ, Schoenfeld MA. Direct neurophysiological evidence for spatial suppression surrounding the focus of attention in vision. *PNAS* 103: 1053-1058, 2006. doi: 10.1073/pnas.0507746103.

Horton JC, Hoyt WF. The representation of the visual field in human striate cortex. *Arch Ophthalmol* 109: 816-824, 1991.

Hubel DH, Livingstone MS. Segregation ofform, color, and stereopsis in primate area 18. *J Neurosci* 7: 3378-3415, 1987.

Hubel DH, Wiesel TN. Laminar and columnar distribution of geniculo-cortical fibers in the macaque monkey. *J Comp Neurol* 146: 421-450, 1972.

Hubel DH, Wiesel TN. Receptive fields, binocular interaction and functional architecture in the cat's visual cortex. *J Physiol* 160: 106-154, 1962.

Huerta MF, Krubitzer LA, Kaas JH. Frontal eye field as defined by intracortical microstimulation in squirrel monkeys, owl monkeys, and macaque monkeys. II. Cortical connections. *J Comp Neurol* 265: 332-361, 1987. doi: 10.1002/cne.902650304.

Huk AC, Heeger DJ. Pattern-motion responses in human visual cortex. *Nat Neurosci* 5: 72-75, 2002.

Huk AC, Ress D, Heeger DJ. Neuronal basis of the motion aftereffect reconsidered. *Neuron* 32: 161-172, 2001.

Ichikawa M, Masakura Y, Munechika K. Dependence of illusory motion on directional consistency in oblique components. *Perception* 35: 933-946, 2006. doi: 10.1068/p5125.

Ignashchenkova A, Dicke PW, Haarmeier T, Thier P. Neuron-specific contribution of the superior colliculus to overt and covert shifts of attention. *Nat Neurosci* 7: 56-64, 2004.

Igusa Y, Sasaki S, Shimazu H. Excitatory premotor burst neurons in the cat pontine reticular formation related to the quick phase of vestibular nystagmus. *Brain Res* 182: 451-456, 1980.

Itti L, Koch C. Computational modeling of visual attention. *Nat. Rev. Neurosci.* 2: 194–203, 2001.

Izawa Y, Suzuki H, Shinoda Y. Response properties of fixation neurons and their location in the frontal eye field in the monkey. *J Neurophysiol* 102: 2410-2422, 2009. doi: 10.1152/jn.00234.2009.

Izawa Y, Suzuki H, Shinoda Y. Suppression of visually and memory-guided saccades induced by electrical stimulation of the monkey frontal eye field. II. Suppression of bilateral saccades. *J Neurophysiol* 92: 2261-2273, 2004. doi: 10.1152/jn.00085.2004.

James W. *Principles of Psychology*, Dover Publications, 1890.

Jeon BB, Swain AD, Good JT, Chase SM, Kuhlman SJ. Feature selectivity is stable in primary visual cortex across a range of spatial frequencies. *Sci Rep* 8: 15288, 2018.

Kafaligonul H. Vision: A systems neuroscience perspective. *J Neurobehav Sci* 1: 21-25, 2014.

Kanwisher N, McDermott J, Chun M. The fusiform face area: a module in human extrastriate cortex specialized for face perception. *J Neurosci* 17: 4302-4311, 1997.

Kardon RH. Anatomy and physiology of the autonomic nervous system. In: *Wash and Hoyt's Clinical Neuro-Ophthalmology*, edited by Miller NR, Newman NJ, Biousse V, and Kerrison JB, 6th ed., p. 649-714, 2005.

Kehoe DH, Aybulut S, Fallah M. Higher order, multifeatural object encoding by the oculomotor system. *J Neurophysiol* 120: 3042-4062, 2018a. doi: 10.1152/jn.00834.2017.

Kehoe DH, Rahimi M, Fallah M. Perceptual color space representations in the oculomotor system are modulated by surround suppression and biased selection. *Front Syst Neurosci* 12: 1, 2018b. doi: 10.3389/fnsys.2018.00001.

Keller EL. Oculomotor specificity within subdivisions of the brain stem reticular formation. In: *The Reticular Formation Revisited*, edited by Hobson JA and Brazier MAB. New York: Raven, p. 227–240, 1980.

King WM, Fuchs AF, Magnin M. Vertical eye movement-related responses of neurons in midbrain near interstitial nucleus of Cajal. *J Neurophysiol* 46: 549-562, 1981.

King WM, Lisberger SG, Fuchs AF. Oblique saccadic eye movements of primates. *J Neurophysiol* 56: 769–784, 1986.

Koch C, Ullman S. Shifts in selective visual attention: Towards the underlying neural circuitry. *Human Neurobiol* 4: 219-227, 1985.

Krauzlis RJ, Lovejoy LP, Ze´non A. Superior colliculus and visual spatial attention. *Annu Rev Neurosci* 36: 165-182, 2013.

Kravitz DJ, Saleem KS, Baker CI, Mishkin M. A new neural framework for visuospatial processing. *Nat Rev Neurosci* 12: 217-230, 2011. doi: 10.1038/nrn3008.

Laeng B, Sirois S, Gredebäck G. Pupillometry: a window to the preconscious? *Perspect Psychol Sci* 7:18–27, 2012. doi: 10.1177/1745691611427305.

Lee PH, Helms MC, Augustine GJ, Hall WC. Role of intrinsic synaptic circuitry in collicular sensorimotor integration. *Neurobiol* 94: 13299-13304, 1997.

Lehmann SJ, Corneil BD. Transient pupil dilation after subsaccadic microstimulation of primate frontal eye fields. *J Neurosci* 36: 3765-3776, 2016. doi: 0.1523/JNEUROSCI.4264-15.2016.

Leichnetz GR, Smith DJ, Spencer RF. Cortical projections to the paramedian tegmental and basilar pons in the monkey. *J Comp Neurol* 228: 388–408, 1984. doi: 10.1002/cne.902280307.

Livingstone M, Hubel D. Anatomy and physiology of a color system in the primate visual cortex. *J Neurosci* 4: 309-356, 1984.

Livingstone M, Hubel D. Segregation of form, color, movement, and depth: Anatomy, physiology, and perception. *Science* 240: 740-749, 1988.

Loewenfeld I. The pupil: Anatomy, physiology, and clinical applications. Detroit: Wayne State UP, 1993.

Luck SJ, Vogel EK. The capacity of working memory for features and conjunctions. *Nature* 390: 279-281, 1997.

Ludwig CJ, Gilchrist ID. Target similarity affects saccade curvature away from irrelevant onsets. *Exp Brain Res* 152: 60-69, 2003. doi: 10.1007/ s00221-003-1520-7.

Lund JS, Boothe R. Interlaminar connections and pyramidal neuron organization in the visual cortex, area 17, of the macaque monkey. *J Comp Neurol* 159: 305-334, 1975.

Mathôt S, van der Linden L, Grainger J, Vitu F. The pupillary light response reveals the focus of covert visual attention. *PLoS ONE*. 8: e78168, 2013.

McDougal DH, Gamlin PDR. Pupillary control pathways. In: *The senses: A comprehensive reference*, edited by Masland RH and Albright T. San Diego: Academic Press, p. 521-536, 2008.

McIlwain JT. Point images in the visual system: New interest in an old idea. *Trends in Neurosciences* 9: 354-358, 1986.

McPeek RM. Incomplete suppression of distractor-related activity in the frontal eye field results in curved saccades. *J Neurophysiol* 96: 2699-2711, 2006. doi: 10.1152/jn.00564.2006.

McPeek RM, Han JH, Keller EL. Competition between saccade goals in the superior colliculus produces saccade curvature. *J Neruphysiol* 89: 2577-2590, 2003. doi: 10.1152/jn.00657.2002.

McPeek RM, Keller EL. Saccade target selection in the superior colliculus during a visual search task. *J Neurophysiol* 88: 2019-2034, 2002.

McPeek RM, Keller EL. Short-term priming, concurrent processing, and saccade curvature during a target selection task in the monkey. *Vision Res* 41: 785–800, 2001.

McSorley E, Haggard P, Walker R. Distractor modulation of saccade trajectories: Spatial separation and symmetry effects. *Exp Brain Res* 155: 320-333, 2004. doi: 10.1007/s00221-003-1729-5.

McSorley E, Haggard P, Walker R. Time course oculomotor inhibition revealed by saccade trajectory modulation. *J Neurophysiol* 96: 1420-1424, 2006. doi: 10.1152/jn.00315.2006.

Miller EK, Li L, Desimone R. Activity of neurons in anterior inferior temporal cortex during a short-term memory task. *J Neurosci* 13: 1460-1478, 1993.

Milner AD, Goodale MA. Two visual systems re-viewed. *Neuropsychologia* 46: 774-785, 2008.

Milner AD, Goodale MA. The visual brain in action. Oxford: Oxford Univ. Press, 1995.

Minken AWH, Van Opstal AJ, Van Gisbergen JAM. Three-dimensional analysis of strongly curved saccades elicited by double-step stimuli. *Exp Brain Res* 93: 521–533, 1993.

Moehler T, Fiehler K. Inhibition in movement plan competition: reach trajectories curve away form remembered and task-irrelevant present but not from task-irrelevant past visual stimuli. *Exp Brain Res* 235: 3251-3260, 2017. doi: 10.1007/s00221-017-5051-z.

Moore T, Armstrong KM, Fallah M. Visuomotor origins of covert spatial attention *Neuron* 40: 671-683, 2003.

Moore T, Fallah M. Control of eye movements and spatial attention. *PNAS* 98: 1273-1276, 2001. doi: 10.1073/pnas.021549498.

Moore T, Fallah M. Microstimulation of the frontal eye field and its effects on covert spatial attention. *J Neurophysiol* 91: 152-162, 2004. doi: 10.1152/jn.00741.2002.

Mulckhuyse M, Van der Stigchel S, Theeuwes J. Early and late modulation of saccade deviations by target distractor similarity. *J Neurophysiol* 102: 1451–1458, 2009. doi: 10.1152/jn.00068.2009.

Müller NG, Kleinschmidt A. The attentional ‘spotlight’s’ penumbra: Center-surround modulation in striate cortex. *NeuroReport* 15: 997-980, 2004. doi: 10.1097/01.wnr.0000125047.66941.17.

Muri RM, Nyffeler T. Neurophysiology and neuroanatomy of reflexive and volitional saccades as revealed by lesion studies with neurological patients and transcranial magnetic stimulation (TMS). *Brain Cogn* 68: 284-292, 2008. doi: 10.1016/j.bandc.2008.08.018.

Optican LM. The role of omnipause neurons: Why glycine? *Prog Brain Res* 171: 115-121, 2008. doi: 10.1016/S0079-6123(08)00615-8.

Pan Y, Wang L, Wang Z, Xu C, Yu W, Spillmann L, Gu Y, Wang Z, Wang W. Representation of illusory and physical rotations in human MST: A cortical site for the pinna illusion, *Hum Brain Mapp* 37: 2097-2113, 2016. doi: 10.1002/hbm.23156.

Pasupathy A, Connor CE. Responses to contour features in macaque area V4. *J Neurophysiol* 82: 2490-2502, 1999. doi: 10.1152/jn.1999.82.5.2490.

Perry CJ, Fallah M. Feature integration and object representations along the dorsal stream visual hierarchy. *Front Comp Neurosci* 8: 84, 2014. doi: 10.3389/fncom.2014.00084.

Port NL, Wurtz RH. Sequential activity of simultaneously recorded neurons in the superior colliculus during curved saccades. *J Neurophysiol* 90: 1887-1903, 2003. doi: 10.1152/jn.01151.2002.

Port NL, Wurtz RH. Two electrode recordings in monkey superior colliculus during curved saccades. *Soc Neurosci Abstr* 26: 297, 2000.

Price NSC, Born RT. Representation of movement. *Encyclopedia of Neuroscience* 8: 107-114, 2009.

Quaia C, Pare M, Wurtz RH, Optican LM. Extent of compensation for variations in monkey saccadic eye movements. *Exp Brain Res* 132: 39–51, 2000.

Rajkowski J, Kubiak P, Aston-Jones G. Correlations between locus coeruleus (LC) neural activity, pupil diameter and behavior in monkey support a role of LC in attention. *Soc Neurosci Abs* 19: 974, 1993.

Rajkowski J, Majczynski H, Clayton E, Aston-Jones G. Activation of monkey locus coeruleus neurons varies with difficulty and performance in a target detection task. *J Neurophysiol* 92: 361-371, 2004.

Recanzone GH, Wurtz R. Shift in smooth pursuit initiation and MT and MST neuronal activity under different stimulus conditions. *J Neurophysiol* 82: 1710-1727, 1999.

Reynolds JH, Chelazzi L. Attentional modulation of visual processing. *Annu Rev Neurosci* 27: 611-647, 2004.

Reynolds JH, Heeger DJ. The normalization model of attention. *Neuron* 61: 168-185, 2009. doi: 10.1016/j.neuron.2009.01.002.

Ro T, Henik A, Machado L, Rafal RD. Transcranial magnetic stimulation of the prefrontal cortex delays contralateral endogenous saccades. *J Cog Neurosci* 9: 433-440, 1997.

Robinson DA. Eye movements evoked by collicular stimulation in the alert monkey. *Vision Res* 12: 1795-1808, 1972.

Robinson DA. The oculomotor control system: A review. *Comp Sci* 56: 1032-1049, 1968.

Robinson DA, Fuchs AF. Eye movements evoked by stimulation of frontal eye fields. *J Neurophysiol* 32: 637-648, 1969.

Roe AW, Chelazzi L, Connor CE, Conway BR, Fujita I, Gallant JL, Lu H, Vanduffel W. Toward a unified theory of visual area V4. *Neuron* 74: 12-29, 2012.

Roelfsema PR. Cortical algorithms for perceptual grouping. *Annu. Rev. Neurosci.* 29: 203-227, 2006. doi: 10.1146/annurev.neuro.29.051605.112939.

Rohrer WH, White JM, Sparks DL. Saccade-related burst cells in the superior colliculus: Relationship of activity with saccadic velocity. *Soc Neurosci Abstr* 13: 1092, 1987.

Saito H, Yukie M, Tanaka K, Hikosaka K, Fukada Y, Iwai E. Integration of direction signals of image motion in the superior temporal sulcus of the macaque monkey. *J Neurosci* 6: 145-157, 1986.

Sakata H, Shibutani H, Ito Y, Tsurugai K, Mine S, Kusunoki M. Functional properties of rotation-sensitive neurons in the posterior parietal association cortex of the monkey. *Exp Brain Res* 101: 183-202, 1994.

Schall JD, Morel A, Kaas JH. Topography of supplementary eye field afferents to frontal eye field in macaque: implications for mapping between saccade coordinate systems. *Vis Neurosci* 10: 385-393, 1993. doi: 10.1017/S0952523800003771.

Schiller PH. The superior colliculus and visual function. In: *Handbook of physiology*, edited by brookhart JM and Mountcastle VB. Philadelphia: Lippincott Williams and Wilkins, p. 457-505, 1984.

Schnupp JWH, Mrsic-Flogel TD, King AJ. Linear processing of spatial cues in primary auditory cortex. *Nature* 414: 200-204, 2001.

Segraves MA. Activity of monkey frontal eye field neurons projecting to oculomotor regions of the pons. *J Neurophysiol* 68: 1967-1985, 1992.

Serences JT, Yantis S. Selective visual attention and perceptual coherence. *Trends Cogn. Sci.* 10:

38–45, 2006. doi: 10.1016/j.tics.2005.11.008.

Sheliga BM, Riggio L, Rizzolatti G. Spatial attention and eye movements. *Exp Brain Res* 105: 261-275, 1995.

Shipp S, Zeki S. Segregation of pathways leading from area V2 to areas V4 and V5 macaque monkey visual cortex, *Nature* 315: 322-325, 1985.

Shipp S, Zeki S. The functional organization of area V2, I: Specialization across stripes and layers. *Vis Neurosci* 19: 187-210, 2002. doi: 10.1017.S0952523802191164.

Sparks DL. The brainstem control of saccadic eye movements. *Nat Rev Neurosci* 3: 952-964, 2002.

Sparks DL, Hartwich-Young R. The deep layers of the superior colliculus. *Rev Oculomot Res* 3: 213-255, 1989.

Sparks DL, Mays LE. Signal transformations required for the generation of saccadic eye movements. *Ann Rev Neurosci* 13:309-336, 1990.

Spencer RF, Wenthold RJ, Baker R. Evidence for glycine as an inhibitory neurotransmitter of vestibular, reticular, and prepositus hypoglossi neurons that project to the cat abducens nucles. *J Neurosci* 9: 2718-2736, 1989.

Stanton GB, Bruce CJ, Goldberg ME. Topography of projections to posterior cortical areas from the macaque frontal eye fields. *J Comp Neurol* 353: 291-305, 1995. doi: 10.1002/cne.903530210.

Stanton GB, Bruce CJ, Goldberg ME. Topography of projections to the frontal lobe from the macaque frontal eye fields. *J Comp Neurol* 330: 286-301, 1993. doi: 10.1002/cne.903300209.

Stanton GB, Goldberg ME, Bruce CJ. Frontal eye field efferents in the macaque monkey: I. Subcortical pathways and topography of striatal and thalamic terminal fields. *J Comp Neurol* 271: 473-492, 1988. doi: 10.1002/cne.902710402.

Steinmetz NA, Moore T. Lumping and splitting the neural circuitry of visual attention. *Neuron* 73: 410-412, 2012.

Störmer VS, Alvarez GA. Feature-based attention elicits surround suppression in feature space. *Curr Bio* 24: 2985-2988, 2014. doi: 10.1016/j.cub.2014.07.030.

Strassman A, Highstein SM, McCrea RA. Anatomy and physiology of saccadic burst neurons in the alert squirrel monkey. I. Excitatory burst neurons. *J Comp Neurol* 249: 337-357, 1986.

Tanaka K. Columns for complex visual object features in the inferotemporal cortex: Clustering of cells with similar but slightly different stimulus selectivities. *Cereb Cortex* 13: 90-99, 2003.

Tang R, Song Q, Li Y, Zhang R, Cai X, Lu HD. Curvature-processing domains in primate V4. *eLife* 9: e57502, 2020. doi: 10.7554/eLife.57502.

Tkacz-Domb S, Yeshurun Y. The size of the attentional window when measured by the pupillary response to light. *Nature* 8: 11878, 2018. doi: 10.1038/s41598-018-30343-7.

Tehovnik EJ, Sommer MA, Chou I, Slocum WM, Schiller PH. Eye fields in the frontal lobes of primates. *Brain Res Rev* 32: 413-448, 2000.

Theeuwes J, Godijn R. Inhibition-of-return and oculomotor interference. *Vision Res* 44: 1485-1492, 2004.

Thompson KG, Bichot NP. A visual salience map in the primate frontal eye field. *Prog Brain Res* 147: 251-262, 2005. doi: 10.1016/S0079-6123(04)47019-8.

Thompson KG, Bichot NP, Schall JD. Dissociation of visual discrimination from saccade programming in macaque frontal eye field. *J Neurophysiol* 77: 1046-1050, 1997.

Tian JR, Lynch JC. Corticocortical input to the smooth and saccadic eye movement subregions of the frontal eye field in Cebus monkeys. *J Neurophysiol* 76: 2754-2771, 1996.

Tombu M, Tsotsos JK. Attending to orientation results in an inhibitory surround in orientation space. *Atten Percept Psychophys* 70: 30-35, 2008. doi: 10.3758/PP.70.1.30.

Tootell RB, Reppas JB, Dale AM, Look RB, Sereno MI, Malach R, Brady TJ, Rosen BR. Visual motion aftereffect in human cortical area MT revealed by functional magnetic resonance imaging. Nature 375: 139-141, 1995.

Tsotsos JK. Analyzing vision at the complexity level. *Behav Brain Sci* 13: 423-469, 1990.

Tsotsos JK, Culhane SM, Yan Kei Wai W, Lai Y, Davis N, Nuflo F. Modeling visual attention via selective tuning. *Artif Intell* 78: 507-545, 1995.

Tsotsos JK, Liu Y, Martinez-Trujillo JC, Pomplun M, Simine E, Zhou K. Attending to visual motion. *Comput Vis Image Underst* 100: 3-40, 2005. doi: 10.1016/j.cviu.2004.10.011.

Van der Stigchel S, Meeter M, Theeuwes J. The spatial coding of the inhibition evoked by distractors. *Vision Res* 47: 210-218, 2007. doi: 10.1016/j.visres.2006.11.001.

Van Gisbergen JAM, Van Opstal AJ, Roebroek JGH. Stimulus induced midflight modification of saccades. In: *Eye Movements: From Physiology to Cognition,* edited by O'Regan JK and Levy-Schoen A. Amsterdam: Elsevier, p. 27–36, 1987.

Van Gisbergen JAM, Van Opstal AJ, Schoenmakers JJ. Experimental test of two models for the generation of oblique saccades. *Exp Brain Res* 57: 321–336, 1985.

Vernet M, Quentin R, Chanes L, Mitsumasu A, Valero-Cabré A. Frontal eye field, where art thou? Anatomy, function, and non-invasive manipulation of frontal regions involved in eye movements and associated cognitive operations. *Front Integr Neurosci* 8: 66, 2014. doi: 10.3389/fnint.2014.00066.

Viviani P, Berthoz A, Tracey D. The curvature of oblique saccades. *Vision Res* 17: 661–664, 1977.

Walker R, McSorley E, Haggard P. The control of saccade trajectories: Direction of curvature depends on prior knowledge of target location and saccade latency. *Atten Percept Psychophys* 68: 129-138, 2006.

Walker R, Techawachirakul P, Haggard P. Frontal eye field stimulation modulates the balance of salience between target and distractors. *Brain Res* 1270: 54-63, 2009. doi: 10.1016/j.brainres.2009.02.081.

Wang CA, Boehnke SE, Itti L, Munoz DP. Transient pupil response is modulated by contrast-based saliency. *J Neurosci* 34: 408-417, 2014. doi: 10.1523/JNEUROSCI.3550-13.2014.

Wang CA, Boehnke SE, White BJ, Munoz DP. Microstimulation of the monkey superior colliculus induces pupil dilation without evoking saccades. *J Neurosci* 32: 3629-3636, 2012. doi: 10.1523/JNEUROSCI.5512-11.2012.

Wang CA, Brien DC, Munoz DP. Pupil size reveals preparatory processes in the generation of pro-saccades and anti-saccades. *Eur J Neurosci* 41: 1102-1110, 2015. doi: 10.1111/ejn.12883.

Wang Q, Burkhalter A. Stream-related preferences of inputs to the superior colliculus from areas of dorsal and ventral streams of mouse visual cortex. *J Neurosci* 33: 1696-1705, 2013. doi: 10.1523/JNEUROSCI.3067-12.2013.

White BJ, Berg DJ, Kan JY, Marino RA, Itti L, Munoz DP. Superior colliculus neurons encode a visual saliency map during free viewing of natural dynamic video. *Nat Commun* 8:14263, 2017. doi: 10.1038/ncomms14263.

White BJ, Boehnke SE, Marino RA, Itti L, Munoz DP. Color-related signals in the primate superior colliculus. *J Neurosci* 29: 12159-12166, 2009. doi: 10.1523/JNEUROSCI.1986-09.2009.

White BJ, Munoz DP. Separate visual signals for saccade initiation during target selection in the primate superior colliculus. *J Neurosci* 31: 1570-1578, 2011.

White BJ, Theeuwes J, Munoz DP. Interaction between visual- and goal-related neuronal signals on the trajectories of saccadic eye movements. *J Cog Neurosci* 24: 707-717, 2012.

Wolfe JM. Guided Search 2.0, A revised model of visual search. *Psychon. Bull. Rev.* 1: 202–238, 1994.

Wolfe JM. The parallel guidance of visual attention. *Curr. Dir. Psychol. Sci.* 1: 125–128, 1992.

Wurtz RH, Goldberg ME. Activity of superior colliculus in behaving monkey: III. Cells discharging before eye movements. *J Neurophysiol* 35: 575-586, 1972.

Yoo SA, Tsotsos JK, Fallah M. The attentional suppressive surround: Eccentricity, location-based and feature-based effects and interactions. *Front Neurosci* 12: 710, 2018. doi: 10.3389/fnins.2018.00710.

Zeki S, Watson JDG, Lueck CJ, Friston KJ, Kennard C, Frackowiak RSJ. A direct demonstration of functional specialization in human visual cortex. *J Neurosci* 11: 641-649, 1973.